CHAPTER 1

Introduction

Heegaard Floer homology is an invariant of closed, oriented three-manifolds, defined by Ozsváth and Szabó by adapting methods from symplectic geometry to Heegaard diagrams [**174**]. Knot Floer homology is a variation of this construction, discovered in 2003 by Ozsváth and Szabó [**172**] and independently by Jacob Rasmussen [**191**], giving an invariant for knots and links in three-manifolds. It is the homology of a chain complex whose generators can be easily read off from a Heegaard diagram, and whose differential counts pseudo-holomorphic disks. Thanks to the contributions of many researchers, the resulting theory has evolved into an active and successful tool for studying knots, links, and three-manifolds.

In 2006, Sucharit Sarkar found a method that rendered some of the pseudo-holomorphic disk counts in the Heegaard Floer differential combinatorial; this was further pursued in a joint paper with Jiajun Wang [**206**]. Inspired by these ideas, Ciprian Manolescu, Ozsváth, and Sarkar [**135**] found a class of Heegaard diagrams for explicitly computing knot Floer homology for knots and links in S^3. These Heegaard diagrams are naturally associated to *grid diagrams*, which are simple combinatorial presentations of knots in S^3, dating back to the 19^{th} century [**17**]. In fact, the above reformulation of knot Floer homology can be used as a *definition* of invariants of knots in S^3: their invariance can also be verified using elementary methods, following the paper of Manolescu, Ozsváth, Szabó, and Dylan Thurston [**136**]. To emphasize this simplicity of the definition, we will call the resulting theory the *grid homology* for knots and links, to distinguish it from its holomorphic antecedent. Of course, grid homology is isomorphic to knot Floer homology; but owing to its elegance and simplicity, grid homology deserves a purely self-contained treatment. This is the goal of the present book.

Before describing the contents of this book in detail, we explain the key features of grid homology.

1.1. Grid homology and the Alexander polynomial

Grid homology is defined in terms of a *grid presentation* of a knot. Such a presentation is given by an $n \times n$ grid of squares, n of which are marked with an O and n of which are marked with an X. These are distributed by the rule that each row and each column contains exactly one square marked with an O and exactly one square marked with an X. By connecting the two markings in every row and in every column (orienting the intervals from X to O in the columns and from O to X in the rows) and following the convention that vertical segments pass over horizontal ones, a grid $\mathbb{G}$ gives rise to a projection of a knot or link together with an orientation on it. In this case we say that $\mathbb{G}$ is a grid presentation of the knot or link. In fact, it is not hard to see that any link type can be presented in this way, cf. Figure 1.1.

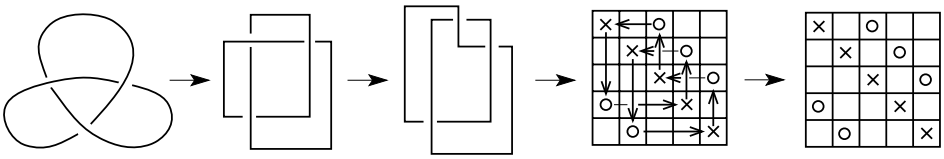

FIGURE 1.1. **Grid diagram of a knot from its projection.** We approximate the diagram by one that involves only horizontal and vertical segments, adjust crossings where horizontal passes over vertical, and mark the turns by O's and X's in an alternating fashion, resulting in a grid diagram.

The simplest version of grid homology for a knot K in S^3, $\widehat{GH}(K)$, is a finite-dimensional, bigraded vector space over the field $\mathbb{F} = \mathbb{Z}/2\mathbb{Z}$ of two elements. This means that $\widehat{GH}(K)$ is a vector space, equipped with a splitting as a direct sum, indexed by pairs of integers:

$$\widehat{GH}(K) = \bigoplus_{d,s\in\mathbb{Z}} \widehat{GH}_d(K,s).$$

In the above decomposition the index d is called the "Maslov grading" and the index s is called the "Alexander grading". Grid homology $\widehat{GH}(K)$ is defined as the homology of a bigraded chain complex $(\widehat{GC}(\mathbb{G}), \widehat{\partial})$ associated to a grid presentation $\mathbb{G}$ of the knot K. The underlying vector space $\widehat{GC}(\mathbb{G})$ decomposes as $\bigoplus_{d,s\in\mathbb{Z}} \widehat{GC}_d(\mathbb{G},s)$, and the differential $\widehat{\partial}$ drops Maslov grading by one and preserves Alexander grading, i.e.

$$\widehat{\partial}\colon \widehat{GC}_d(\mathbb{G},s) \to \widehat{GC}_{d-1}(\mathbb{G},s).$$

Thus, both gradings descend to give the stated bigrading on the homology $\widehat{GH}(K)$. The chain complex itself depends on the grid presentation of the knot, but its homology is independent of this choice.

As a simple example, consider the unknot $\mathcal{O}$. It turns out that the grid homology $\widehat{GH}(\mathcal{O})$ has total dimension one, supported in Alexander and Maslov gradings equal to zero; i.e.

$$\widehat{GH}_d(\mathcal{O},s) = \begin{cases} \mathbb{F} & \text{if } d = s = 0 \\ 0 & \text{otherwise.} \end{cases} \tag{1.1}$$

Since grid homology has two gradings, its Poincaré polynomial is naturally a Laurent polynomial in two formal variables q and t:

$$P_K(q,t) = \sum_{d,s\in\mathbb{Z}} \dim_{\mathbb{F}} \widehat{GH}_d(K,s)\cdot t^s q^d. \tag{1.2}$$

The natural *graded Euler characteristic* in this case is a Laurent polynomial in a single indeterminate t, obtained by setting $q = -1$:

$$\chi(\widehat{GH}(K)) = P_K(-1,t) = \sum_{d,s\in\mathbb{Z}} (-1)^d \dim_{\mathbb{F}} \widehat{GH}_d(K,s)\cdot t^s \in \mathbb{Z}[t,t^{-1}].$$

One of the key properties of grid homology is its relationship with a classical polynomial invariant for knots, the *Alexander polynomial*, see [**1**]. This relationship is expressed in the following:

THEOREM 1.1.1. *The graded Euler characteristic of the grid homology of a knot $K \subset S^3$ coincides with the (symmetrized) Alexander polynomial $\Delta_K(t)$ of K:*

$$\chi(\widehat{GH}(K)) = \Delta_K(t).$$

The Alexander polynomial of a knot satisfies a number of basic properties. We recall some of these below:

(A-1) It is symmetric in t; i.e. $\Delta_K(t) = \Delta_K(t^{-1})$.
(A-2) It is invariant under taking the mirror image of the knot; i.e. if $m(K)$ denotes the mirror of K, then $\Delta_K(t) = \Delta_{m(K)}(t)$.
(A-3) Evaluating the Alexander polynomial at $t = 1$ gives the value 1.
(A-4) The Alexander polynomial satisfies a "skein relation", which relates the Alexander polynomials of two knots K_+ and K_- that differ in a single crossing change, and the Alexander polynomial of the two-component link K_0 obtained by taking the oriented resolution at the crossing:

$$\Delta_{K_+}(t) - \Delta_{K_-}(t) = (t^{\frac{1}{2}} - t^{-\frac{1}{2}})\Delta_{K_0}(t).$$

(The third term here uses a natural extension of the Alexander polynomial to oriented links in S^3. Notice that our convention for the Alexander polynomial differs from the convention used in [**119**] by a multiplicative factor of $(-1)^{|L|-1}$, where $|L|$ denotes the number of components of the link L.)

These results have analogues in grid homology. For example, there are symmetries between grid homology groups generalizing Properties (A-1) and (A-2) (see Propositions 7.1.1 and 7.1.2 respectively). Property (A-3) has a manifestation in grid homology (see Proposition 6.1.4) which is used in the construction of an integer-valued invariant $\tau(K)$, which we will discuss in the next section. Perhaps the most interesting of the above properties is the skein relation, Property (A-4). The analogue of this result is a "skein exact sequence" which is a long exact sequence relating the grid homology groups $\widehat{GH}$ of K_+, K_-, and K_0, where the third term uses a version of grid homology for links. For the exact sequence of grid homologies, see Theorems 9.1.1 and 9.1.2.

1.2. Applications of grid homology

Grid homology is useful, for example, in the study of three numerical invariants of knots: the Seifert genus, the slice genus, and the unknotting number. A knot K in S^3 bounds embedded, oriented, compact surfaces (such a surface is called a *Seifert surface* of K), and the minimal genus of such a surface is the *Seifert genus* $g(K)$ of K. A smoothly embedded, oriented, compact surface $(F, \partial F) \to (D^4, \partial D^4 = S^3)$ in the four-ball D^4 with the property that $\partial F = K$ is called a *slice surface* for K. By taking the minimum of the genera of slice surfaces of K, we arrive at an inherently four-dimensional invariant, the *slice genus* (or *four-ball genus*) $g_s(K)$ of K. The *unknotting number* of a knot K is the minimum number of times the knot needs to pass through itself to obtain the unknot. The following inequalities are easily verified: $g_s(K) \leq g(K)$ and $g_s(K) \leq u(K)$.

Common features of the slice genus and the unknotting number are that both can be easily bounded from above, but both are difficult to compute. For example, for the (p, q) torus knot, it is straightforward to find an unknotting with $\frac{(p-1)(q-1)}{2}$ crossing changes. John Milnor conjectured in 1968 [**144**] that this bound is sharp.

This conjecture was verified by Peter Kronheimer and Tomasz Mrowka in 1993 [**106**] using smooth four-manifold topology and, specifically, the four-manifold invariants introduced by Simon Donaldson [**34**]:

THEOREM 1.2.1 (Kronheimer-Mrowka, [**106**]). *Both the unknotting number and the slice genus of the (p, q) torus knot $T_{p,q}$ are equal to $\frac{(p-1)(q-1)}{2}$.* □

The original proof of the above theorem is based on a stronger result, the *generalized Thom conjecture*, that concerns the minimal genus problem in a smooth Kähler surface. After this breakthrough, a number of other proofs have emerged, using Seiberg-Witten theory [**107, 150**] and Heegaard Floer homology [**168**]. Other proofs of Theorem 1.2.1 have been found using knot Floer homology [**170, 191**] and Khovanov homology [**194**].

Following work of Sarkar [**204**], grid homology can also be used to give a self-contained proof of Theorem 1.2.1, as follows. First, by attaching further structures to grid homology, we obtain a variant $GH^-(K)$ of the construction, which is a bigraded module over the polynomial algebra $\mathbb{F}[U]$ in an indeterminate U. This bigraded module encodes an integer invariant $\tau(K)$ for knots. In Chapter 6, we present a simple proof of the inequality

$$|\tau(K)| \leq u(K), \tag{1.3}$$

which quickly leads to a proof of the Milnor conjecture for torus knots. In Chapter 8, this inequality is sharpened, to give

$$|\tau(K)| \leq g_s(K), \tag{1.4}$$

leading to a proof of Theorem 1.2.1.

The invariant τ can also be used to find knots with trivial Alexander polynomial that have $g_s(K) > 0$. Combining the existence of such knots with work of Michael Freedman [**59, 60**], exotic differentiable structures on $\mathbb{R}^4$ can be constructed; see Section 8.6. (The first examples of exotic differentiable structures on $\mathbb{R}^4$ were discovered by combining work of Donaldson [**33**] and Freedman [**59**]; cf. [**30, 76**].)

In a different direction, grid homology can be used to effectively study contact geometric properties of knots in the standard three-sphere. Recall that a *contact structure* on a three-manifold is a two-plane field ξ that is nowhere integrable. More formally, it is the kernel of a one-form α with the property that $\alpha \wedge d\alpha$ is a volume form. There is a canonical contact structure on $\mathbb{R}^3$, specified by the one-form $\alpha = dz - y\,dx$, which naturally extends to the one-point compactification S^3. The contact structure on $\mathbb{R}^3$ is canonical in the sense that every contact structure in dimension three is locally contactomorphic to this standard model.

There are two natural variations on knot theory one can study in the presence of a contact structure. One of these is *Legendrian knot theory*, where one considers *Legendrian knots*, which are smoothly embedded knots everywhere tangent to ξ. Two such knots are considered equivalent if they are isotopic via a one-parameter family of Legendrian knots. Another variation of knot theory in a contact manifold is provided by *transverse knots*, i.e. by knots that are everywhere transverse to the two-plane field ξ. These are then studied up to transverse isotopy. (For further background on these notions, see Chapter 12.)

Besides their smooth knot types, Legendrian knots come with two further "classical" numerical invariants, their Thurston-Bennequin and rotation numbers. A motivating problem of Legendrian knot theory is to understand to what extent

these invariants determine the Legendrian knot type. A smooth knot type is said to be *(Legendrian) non-simple* if it contains Legendrian non-isotopic pairs of knots with identical classical invariants. Building on work of Yasha Eliashberg, Alexander Givental and Helmut Hofer [**40**], Yuri Chekanov [**23**] produced the first pair of such Legendrian knots.

Unlike Legendrian knots, transverse knots have only one classical numerical invariant, their self-linking number. The definition of Legendrian non-simplicity naturally adapts to the transverse setting: a knot type is *transversely non-simple* if it contains two transverse knots with equal self-linking numbers which are not transversely isotopic. Examples of transversely non-simple knot types were given by John Etnyre and Ko Honda using convex surface theory [**47**], see also [**13**].

The connection of Legendrian and transverse knot theory with grid homology is provided by the following observation: grid position naturally realizes the underlying knot as a Legendrian knot in the standard contact three-sphere. Moreover, the grid complex associated to a given grid diagram comes equipped with two canonical cycles, whose homology classes give invariants of the Legendrian knot type. Similarly, a grid diagram naturally defines a transverse knot, and one of the two cycles above provides a transverse invariant. With the use of these invariants, results of Chekanov and Etnyre-Honda can be reproved in a fairly simple manner, following [**185**] and [**25, 102, 157**] respectively. Specifically, in Sections 12.4 and 12.6, we will prove the following two theorems:

THEOREM 1.2.2 (Chekanov [**23**]). *The knot type $m(5_2)$ shown in Figure 1.2 is Legendrian non-simple.* □

THEOREM 1.2.3 (Etnyre-Honda [**47**]). *There are transversely non-simple knot types in S^3.* □

While Etnyre and Honda verified transverse non-simplicity for a certain cable of the trefoil knot [**47**], in this book we will show transverse non-simplicity of several other simpler knot types, including $m(10_{132})$ shown in Figure 1.3. This latter knot was shown to be transversely non-simple in [**157**]; our presentation will also draw on the argument from [**102**].

1.3. Knot Floer homology

Grid homology is a special case of a holomorphic construction of an earlier-defined invariant, *knot Floer homology* $\widehat{\mathrm{HFK}}$ and HFK^- [**172, 191**]. Grid diagrams

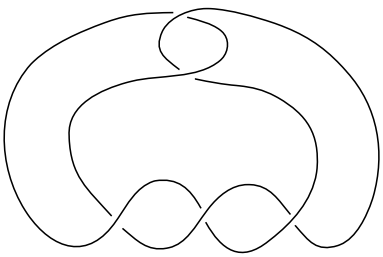

FIGURE 1.2. **The twist knot $m(5_2)$.** This is the knot with smallest crossing number which is Legendrian non-simple. It is the mirror image of the knot type 5_2 from [**198**].

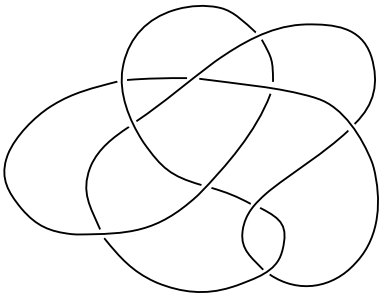

FIGURE 1.3. **The knot** $m(10_{132})$, the mirror image of the knot 10_{132} of Rolfsen's table [**198**]. This knot type contains transverse knots which are not transversely isotopic, although have equal self-linking numbers.

allow us to bypass the technically more involved theory of pseudo-holomorphic curves central to knot Floer homology. The price is that the present approach appears to be too rigid to verify some of the results that are accessible with the strength of the whole theory. To put grid homology in context, we collect some important results of knot Floer homology here. (Below we will refer to knot Floer homology with coefficients in $\mathbb{F} = \mathbb{Z}/2\mathbb{Z}$.)

A key feature of knot Floer homology, proved using the holomorphic theory, states that it recognizes the unknot, in the sense that:

THEOREM 1.3.1 ([**171**]). *The knot Floer homology* $\widehat{\mathrm{HFK}}(K)$ *of a knot* $K \subset S^3$ *has total dimension equal to one if and only if* K *is the unknot* $\mathcal{O}$. □

The above theorem follows from a more general result, which states that knot Floer homology detects the Seifert genus $g(K)$ of a knot K. To state it, note that knot Floer homology $\widehat{\mathrm{HFK}}$ is bigraded, i.e. it is given with a splitting

$$\widehat{\mathrm{HFK}}(K) = \bigoplus_{d,s\in\mathbb{Z}} \widehat{\mathrm{HFK}}_d(K,s),$$

so that its graded Euler characteristic is the Alexander polynomial.

THEOREM 1.3.2 ([**171**]). *If* $K \subset S^3$ *is a knot, then the Seifert genus of* K *is equal to the maximal integer* s *for which* $\widehat{\mathrm{HFK}}_*(K,s)$ *is non-zero.* □

(In [**171**], the above result was stated using $\widehat{\mathrm{HFK}}$ with $\mathbb{Z}$ coefficients; but the proof immediately adapts to show the same result with $\mathbb{Z}/2\mathbb{Z}$ coefficients, as well.)

A classical property of the Alexander polynomial is that it is monic if K is fibered. The corresponding property for knot Floer homology is fairly straightforward to establish [**175**]. The converse to this result, proved by Paolo Ghiggini in the case where $g(K) = 1$ [**71**] and in general by Yi Ni [**160**], is much deeper and gives the following:

THEOREM 1.3.3 ([**71, 160**]). *If* $K \subset S^3$ *is a knot with Seifert genus* g*, then* $\dim_{\mathbb{F}} \widehat{\mathrm{HFK}}_*(K,g) = 1$ *if and only if* K *is fibered.* □

András Juhász has given alternate proofs of both Theorems 1.3.2 and 1.3.3, using *sutured Floer homology* [**96, 97**].

A knot K is called *alternating* if it admits a diagram with the property that crossings alternate between over- and under-crossings, as we travel along the knot. The study of alternating knots is rather simpler than the general case. In particular, in the alternating case, the Alexander polynomial contains much more information about the knot. If K is alternating then the Alexander polynomial detects whether or not K is the unknot; more generally it encodes the Seifert genus of K; and it also encodes whether or not K is a fibered knot. (For details of this statement, see Theorem 2.4.13.) In fact Theorems 1.3.1, 1.3.2 and 1.3.3 can be viewed as extensions of these results to arbitrary knots, replacing the Alexander polynomial with the Poincaré polynomial of knot Floer homology. Indeed, for an alternating knot K the Poincaré polynomial of $\widehat{\mathrm{HFK}}(K)$ is determined by the Alexander polynomial $\Delta_K(t)$ and the signature $\sigma(K) \in \mathbb{Z}$ of K; we prove the analogous statement for grid homology in Theorem 10.3.1.

In addition to the above topological applications, the flexibility afforded by knot Floer homology makes it amenable to performing computations for certain infinite families of knots, for example, for torus knots (see Theorem 16.2.6).

The definition of knot Floer homology admits a natural extension to knots (and links) in arbitrary closed, oriented three-manifolds. This extension fits into the broader framework of Heegaard Floer homology for three-manifolds [**173, 174**]. Moreover, knot Floer homology is a useful device for computing the Heegaard Floer homology groups of three-manifolds obtained by Dehn surgery on K; see [**181**]. The details of these constructions are, however, beyond the scope of this book.

1.4. Comparison with Khovanov homology

It is interesting to compare the formal structure of knot Floer homology with a different kind of knot invariant defined by Mikhail Khovanov [**103**], and its various generalizations due to Khovanov and Lev Rozansky [**104, 105**]. For the sake of exposition, we focus on the simplest version, from [**103**]; see also [**8, 222**].

Like knot Floer homology, Khovanov homology is a bigraded vector space associated to a knot or link in S^3. Its graded Euler characteristic is another familiar knot polynomial: the *Jones polynomial* [**93**]. Khovanov homology can be enriched by a further differential, introduced by Eun-Soo Lee [**117**]; and Rasmussen [**194**] has used that differential to define a concordance invariant s similar in spirit to τ. These ideas led Rasmussen to give the first combinatorial proof of Theorem 1.2.1.

An analogue of Theorem 1.3.1 holds for Khovanov homology: Kronheimer and Mrowka [**112**] have shown that the unknot is the only knot whose Khovanov homology has dimension two over $\mathbb{Q}$. In fact, it is conjectured that the Jones polynomial also detects the unknot [**94**].

Intriguing though these similarities are, a precise mathematical relationship between the constructions of knot Floer and Khovanov homologies has yet to be discovered; compare [**36, 191**].

In a different direction, it is also interesting to compare knot Floer homology with analogous invariants coming from gauge theory, especially instanton homology for knots [**54, 113**].

1.5. On notational conventions

In the present book, we wish to distinguish properties of knot Floer homology that follow from the holomorphic theory (such as Theorem 1.3.1) from properties

that can be derived purely within the combinatorial framework, and which we will proceed to prove in this book. To help emphasize this point, we make a semantic distinction between knot Floer homology and grid homology; and we make a corresponding notational distinction as well.

For the convenience of the experts, we have assembled a dictionary below connecting the traditional notation for knot Floer homology with the notation for grid homology we use here. The first column describes some construction and, in

The complex for knot/link homology (crossing no basepoints) *Fully blocked grid complex*	$\widetilde{CL}(G)$ [**136**]	$\widetilde{GC}(\mathbb{G})$
Link Floer homology (crossing no basepoints) *Fully blocked grid homology*	$\widetilde{HL}(\vec{L})$ [**136**]	$\widetilde{GH}(\vec{L})$
The knot/link Floer complex (crossing $\mathbb{O}$ basepoints) *Unblocked grid complex*	$\mathrm{CFK}^-(K)$ [**185**]; $\mathrm{CFL}^-(\vec{L})$ [**180**]; $CL^-(G)$ [**136**]	$GC^-(\mathbb{G})$
Knot/link Floer homology (crossing $\mathbb{O}$ basepoints) *Unblocked grid homology*	$\mathrm{HFK}^-(K)$ [**185**]; $\mathrm{HFL}^-(\vec{L})$ [**180**]	$GH^-(\vec{L})$
The complex for knot Floer homology with $U = 0$ *Simply blocked grid complex*	$\widehat{\mathrm{CFK}}(K)$ [**172**]	$\widehat{GC}(\mathbb{G})$
Knot Floer homology with $U = 0$ *Simply blocked grid homology*	$\widehat{\mathrm{HFK}}(K)$ [**172**]	$\widehat{GH}(K)$
Link Floer homology with collapsed grading and with $U = 0$ *Simply blocked, bigraded grid homology for links*	$\widehat{\mathrm{HFK}}(\vec{L})$ [**172**]	$\widehat{GH}(\vec{L})$
Link Floer homology *Simply blocked, multi-graded grid homology for links*	$\widehat{\mathrm{HFL}}(\vec{L})$ [**180**]	$\widehat{\mathbf{GH}}(\vec{L})$
Link Floer homology *Unblocked, multi-graded grid homology for links*	$\mathrm{HFL}^-(\vec{L})$ [**180**]	$\mathbf{GH}^-(\vec{L})$
The filtered knot complex $\widehat{\mathrm{CF}}(S^3)$ (crossing all $\mathbb{X}$ and all but one of the $\mathbb{O}$) *Simply blocked filtered grid complex*	$CFK^{0,*}(S^3, K)$ [**172**]	$\widehat{\mathcal{GC}}(\mathbb{G})$
The filtered knot complex $\mathrm{CF}^-(S^3)$ (crossing all basepoints) *(Unblocked) filtered grid complex*	$CFK^{-,*}(S^3, K)$ [**172**]	$\mathcal{GC}^-(\mathbb{G})$
The multi-filtered link complex (crossing all basepoints) *(Unblocked) filtered grid complex*	$CFL^{-,*}(\vec{L})$ [**180**]	$\boldsymbol{\mathcal{GC}}^-(\mathbb{G})$

italics, gives the name we call it in the present book. In the next column, we give the notation of the concept customary in knot Floer homology and indicate references where the notation is introduced or used extensively. In the final column, we include the notation used in this book.

Link Floer homology is typically thought of as endowed with an Alexander multi-grading. In the text we distinguish the multi-graded versions from their bigraded analogues by using boldface for the multi-graded ones ($\mathbf{GC}^-(\mathbb{G})$, $\widehat{\mathbf{GC}}(\mathbb{G})$, $\mathbf{GH}^-(\vec{L})$, $\widehat{\mathbf{GH}}(\vec{L})$), rather than the usual typeface for their bigraded analogues ($GC^-(\mathbb{G})$, $\widehat{GC}(\mathbb{G})$, $GH^-(\vec{L})$ and $\widehat{GH}(\vec{L})$).

There are two natural conventions for the Maslov grading of a link, which are different when the link has more than one component. In the present work, we made a choice which differs from the choices made elsewhere (e.g. in [**172**]). These two gradings differ by $\frac{\ell-1}{2}$, where ℓ denotes the number of components; see Equation (9.18). Using our present choice, for any link, the Maslov grading is always integer-valued.

1.6. Necessary background

This book is aimed at a wide audience, ranging from motivated undergraduates curious about modern methods in knot theory, to graduate students and researchers who want a leisurely introduction to the combinatorial aspects of Heegaard Floer homology. Some familiarity with knot theory would be helpful, say, on the level of [**28, 119, 198**], though in Chapter 2 this is recalled. The development of grid homology also uses some basic tools from homological algebra: chain complexes, chain maps, chain homotopies, and mapping cones. These concepts can be found in introductory books on algebraic topology such as [**83**]; see also [**226**]. For the reader's convenience, though, the relevant part of homological algebra is briefly summarized either before it is used or in Appendix A.

As we shall see in Chapter 12, Legendrian and transverse knots and links in the standard contact three-sphere lend themselves to study through grids and grid homology. Although we have attempted to make this chapter as self-contained as possible, at times we will refer the reader to basic texts in contact topology, such as [**45, 68**].

1.7. The organization of this book

We start our discussion in Chapter 2 with a short review of the classical theory of knots and links in the three-space. The concept of grid diagrams, their relation to the Alexander polynomial, and to Seifert surfaces are described in Chapter 3. In Chapter 4 we introduce the main object of the book, grid homologies of knots. We start with a simple version and then build up to the further, slightly more complicated variants. The invariance of these homology groups (i.e. independence of the presentation of a knot by a grid diagram) is discussed in Chapter 5.

After setting up the basics of the theory, we turn to the first applications. In Chapter 6 we give a short proof of the fact that the τ-invariant bounds the unknotting number. This result then leads to the verification of Milnor's conjecture on the unknotting numbers of torus knots. Further basic properties are discussed in Chapter 7.

The rest of the book is devoted to more advanced topics in grid homology. In Chapter 8 we strengthen the unknotting bound and show that $|\tau(K)| \leq g_s(K)$,

completing the proof of Theorem 1.2.1. Chapter 9 provides an important computational tool, the skein exact sequence. We also show instances where this long exact sequence can be conveniently used in explicit computations. A variation of the skein exact sequence, presented in Chapter 10, then leads us to the computation of grid homology for all alternating knots. In Chapter 11 we give the details of the extension of grid homology from knots to links. To put this construction into perspective, we also recall some standard facts about the multi-variable Alexander polynomial of a link and the Thurston norm of a link complement. In Chapter 12 we give applications of grid homology for Legendrian and transverse knots. In particular, in Sections 12.4 and 12.6 we prove Theorems 1.2.2 and 1.2.3. Chapter 13 provides further algebraic background and describes a generalization of the invariant, which is the filtered quasi-isomorphism type of a filtered chain complex over an appropriate polynomial ring. In Chapter 14 further properties of the filtered chain complex are discussed. In Chapter 15, we explain the sign conventions required to develop grid homology with coefficients in $\mathbb{Z}$. In Chapter 16 we review some basic aspects of Heegaard Floer homology, a theory initiated in [**173, 174**] and further developed in [**172, 180, 191**] for knots and links in general three-manifolds. We also explain why the combinatorial theory discussed in the earlier chapters is, indeed, a special case of this more general theory. In Chapter 17 we collect some open problems, hopefully motivating further reading and research in the subject. For the sake of completeness, in Appendix A, we include elements of homological algebra which we use throughout the book. The text also uses some basic theorems of knot theory (such as the Reidemeister and the Reidemeister-Singer theorems and Cromwell's theorem on grids). Appendix B is devoted to the proofs of these results.

We have included a number of exercises throughout the text, with varying levels of difficulty. More challenging problems are marked with an asterisk *.

The material presented here is an exposition of results which have already appeared in the literature. Our exposition of basic knot theory was influenced by [**100, 101, 119, 189, 198**]; for grid diagrams we have drawn on [**28, 37**]. Our discussion of grid homology follows the account from [**136**] (see also [**135**]), with further topics coming from [**66, 85, 157, 167, 185, 204, 231**]. The proof of the unknotting bound from Chapter 6 is new, though it is inspired by [**204**]. The proof that grid homology gives bounds on the Seifert genus (Proposition 7.2.2) is new; but our treatment falls short of showing that these bounds are sharp, as we know from the holomorphic theory. The organization of the invariance proof of the grid invariants is a little different from that in [**136**]: we have chosen here to start from the simplest cases (invariance of the grid homology groups with coefficients mod 2) and build up to the general case (for the filtered quasi-isomorphism type), rather than going the other direction, as was done in [**136**]. As a by-product, the invariance proof presented here is somewhat simpler than the proof from [**136**].

This book could be used as a textbook for a semester-long course either at the graduate level or at an advanced undergraduate level. The background is reviewed in Chapter 2 and in Appendix A (especially Sections A.1–A.5). The material developed in Chapters 3-7 could serve as the core for this course. The topics covered in Chapters 8, 9, and the first three sections of Chapter 15 are essentially independent, and any of these could be added as additional topics.

A course with more advanced topics could include the computation of the grid homology for alternating knots from Chapter 10; and the extension of the theory to

links from Chapter 11. Chapter 12 is a further essentially independent discussion on the role of grid homology in contact knot theory. The reader interested in pursuing Heegaard Floer homology further is encouraged to study Chapters 13 and 14 (and to read Chapter 16, as a preview).

1.8. Acknowledgements

The work presented here owes a great deal to the work of other researchers, both in this and in related subjects.

Knot Floer homology is built on Heegaard Floer homology, which in turn grew out of studying Seiberg-Witten gauge theory and Heegaard splittings.

The Seiberg-Witten equations on smooth four-manifolds were introduced by Nathan Seiberg and Edward Witten [**208, 209, 230**], see also [**149**]. Their introduction led to many important applications for smooth four-dimensional topology, and in particular, thanks to the fundamental contributions of Cliff Taubes [**215**], a link between four-manifold topology and Mikhail Gromov's invariants in symplectic geometry [**81**]. It also provided a framework for new three-dimensional invariants. Peter Kronheimer and Tom Mrowka were pioneers in the development of Seiberg-Witten theory for three-manifolds [**110, 111**]. Seiberg-Witten theory, in turn, was formulated as an alternative to Simon Donaldson's invariants for smooth four-manifolds [**35**], constructed using the anti-self-dual Yang-Mills equations. Donaldson's breakthrough formed the foundation of the modern understanding of smooth four-dimensional topology. The corresponding three-manifold invariant was defined and explored by Andreas Floer [**49**], whose work provided further guiding principles in Heegaard Floer homology.

Much of the work presented here is based on joint work with other collaborators. Grid homology was discovered in collaboration with Ciprian Manolescu and Sucharit Sarkar, and further developed in collaboration with Dylan Thurston. Hence our discussion here is heavily influenced by their ideas. Some of the applications of the transverse invariant were found in collaboration with Lenny Ng.

Moreover, the exposition of the solution for the Milnor conjecture we give here was motivated by Sucharit Sarkar's proof [**204**]. Our treatment of grid homology for alternating knots follows the work of Mike Wong [**231**], which in turn rests on earlier work of Ciprian Manolescu [**132**]. Our discussion of the theory over $\mathbb{Z}$ uses ideas of Étienne Gallais [**66**]. Some examples of transversally non-simple knots were taken from work of Lenny Ng and Tirasan Khandhawit [**102**].

We would like to thank the following people for providing valuable input on early drafts of this work: Daniel Copeland, Stefan Friedl, Marco Golla, Robert Lipshitz, Lilya Lyubich, András Szűcs and Mike Wong. We are also very grateful to Robert Lipshitz and Sucharit Sarkar for discussions pertinent to Chapter 17. Many of the figures were created by Boldizsár Kalmár; some others were drawn with the help of Mathematica.

Finally, all three of us owe a great deal to our advisor, John Morgan, who introduced us patiently to modern developments in low dimensional topology when we were graduate students, and has supplied both guidance and friendship in the years since.

During the course of this work Peter Ozsváth was partially supported by NSF DMS-1405114. András Stipsicz was partially supported by the *Lendület program ADT*, ERC Advanced Grant LDTBud and OTKA NK81203, K112735; he would

also like to thank the Institute for Advanced Study in Princeton for its hospitality during much of this work. Zoltán Szabó was partially supported by NSF DMS-1006006 and NSF DMS-1309152.

CHAPTER 4

Grid homology

The aim of the present chapter is to define the chain complexes for computing grid homology, following [**135, 136**]. We define three versions: $\widetilde{GC}(\mathbb{G})$, $\widehat{GC}(\mathbb{G})$, and $GC^-(\mathbb{G})$. The first of these is the simplest, and the first two are both specializations of the last one, which in turn is a specialization of a more complicated algebraic object $\mathcal{GC}^-(\mathbb{G})$ that we will meet in Chapter 13. In this chapter, and in fact, all the way until Chapter 8, we will consider primarily the case of knots.

This chapter is organized as follows. Section 4.1 introduces *grid states*, the generators of the grid chain complexes. Differentials count rectangles in the torus, and in Section 4.2 we describe how rectangles can connect grid states. In Section 4.3, we define two functions, the Maslov function and the Alexander function on grid states; these functions will induce the bigradings on the grid complexes. In Section 4.4 we define the grid complex $\widetilde{GC}$, the variant with the minimal amount of algebraic structure. In Section 4.5, we give a quick overview of some of the basic constructions from homological algebra (chain complexes, chain homotopies, quotient complexes) which will be of immediate use. (For more, see Appendix A.) In Section 4.6, we define further versions of the grid complex GC^- and $\widehat{GC}$. In Section 4.7, we interpret the Alexander function in terms of the winding number, leading to an expression of the Euler characteristic of $\widetilde{GH}$ and $\widehat{GH}$ in terms of the Alexander polynomial. Section 4.8 gives some concrete calculations of grid homology. In Section 4.9, we conclude with some remarks relating the combinatorial constructions with analogous holomorphic constructions.

4.1. Grid states

Consider a toroidal grid diagram for a knot K with grid number n, as described in Section 3.1. Think of each square in the grid as bounded by two horizontal and two vertical arcs. The horizontal arcs can be assembled to form n horizontal circles in the torus, denoted $\boldsymbol{\alpha} = \{\alpha_i\}_{i=1}^n$, and the vertical ones can be assembled to form n vertical circles, denoted $\boldsymbol{\beta} = \{\beta_i\}_{i=1}^n$.

Definition 4.1.1. A ***grid state*** for a grid diagram $\mathbb{G}$ with grid number n is a one-to-one correspondence between the horizontal and vertical circles. More geometrically, a grid state is an n-tuple of points $\mathbf{x} = \{x_1, \dots, x_n\}$ in the torus, with the property that each horizontal circle contains exactly one of the elements of $\mathbf{x}$ and each vertical circle contains exactly one of the elements of $\mathbf{x}$. The set of grid states for $\mathbb{G}$ is denoted $\mathbf{S}(\mathbb{G})$.

A grid state $\mathbf{x}$ can be thought of as a graph of a permutation; i.e. if $\mathbf{x} = \{x_1, \dots, x_n\}$, then $\sigma = \sigma_{\mathbf{x}}$ is specified by the property that $x_i = \alpha_{\sigma(i)} \cap \beta_i$. The correspondence between grid states and permutations is, of course, not canonical: it depends on a numbering of the horizontal and vertical circles.

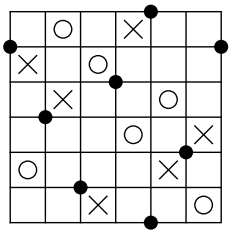

FIGURE 4.1. **A grid state in $\mathbf{S}(\mathbb{G})$.** Labelling the circles from left to right and bottom to top in this picture, the grid state corresponds to the permutation $(1,2,3,4,5,6) \mapsto (6,4,2,5,1,3)$.

When illustrating the diagrams and the states, we use planar grids; that is, cut the toroidal grid along a vertical and a horizontal circle. The square obtained by cutting up the torus is a *fundamental domain* for the torus, and the induced planar grid diagram is the planar realization of the grid diagram. Figure 4.1 illustrates a grid state in a grid diagram for the figure-eight knot. To emphasize the side identifications used in going from the planar to the toroidal grid, we repeat components of the grid state on the left and the right edge, and the top and the bottom edge.

4.2. Rectangles connecting grid states

The chain complexes associated to a grid diagram are generated by grid states, and their differentials count rectangles connecting states. The various versions of the grid complex differ in how they count rectangles. We formalize the concept of connecting rectangles, as follows.

Fix two grid states $\mathbf{x}, \mathbf{y} \in \mathbf{S}(\mathbb{G})$, and an embedded rectangle r in the torus whose boundary lies in the union of the horizontal and vertical circles, satisfying the following relationship. The sets $\mathbf{x}$ and $\mathbf{y}$ overlap in $n-2$ points in the torus, and the four points left out are the four corners of r. There is a further condition stated in terms of the orientation r inherits from the torus. The oriented boundary of r consists of four oriented segments, two of which are vertical and two of which are horizontal. The rectangle r *goes from* $\mathbf{x}$ *to* $\mathbf{y}$ if the horizontal segments in ∂r point from the components of $\mathbf{x}$ to the components of $\mathbf{y}$, while the vertical segments point from the components of $\mathbf{y}$ to the components of $\mathbf{x}$.

More formally, if r is a rectangle, let $\partial_\alpha r$ denote the portion of the boundary of r in the horizontal circles $\alpha_1 \cup \ldots \cup \alpha_n$, and let $\partial_\beta r$ denote the portion of the boundary of r in the vertical ones. The boundary inherits an orientation from r. The rectangle r goes from $\mathbf{x}$ to $\mathbf{y}$ if

$$\partial(\partial_\alpha r) = \mathbf{y} - \mathbf{x} \qquad \text{and} \qquad \partial(\partial_\beta r) = \mathbf{x} - \mathbf{y},$$

where $\mathbf{x} - \mathbf{y}$ is thought of as a formal sum of points; e.g. at points in $p \in \mathbf{x} \cap \mathbf{y}$, the difference cancels.

If there is a rectangle from $\mathbf{x}$ to $\mathbf{y}$, then all but two points in $\mathbf{x}$ must also be in $\mathbf{y}$. This is equivalent to the condition that the associated permutations $\sigma_{\mathbf{x}}$ and $\sigma_{\mathbf{y}}$ satisfy the property that $\sigma_{\mathbf{x}}^{-1} \cdot \sigma_{\mathbf{y}}$.

ξ associated to $\mathbf{x}$ and the permutation η associated to $\mathbf{y}$ are related by the property that $\xi \cdot \eta^{-1}$ is a transposition.

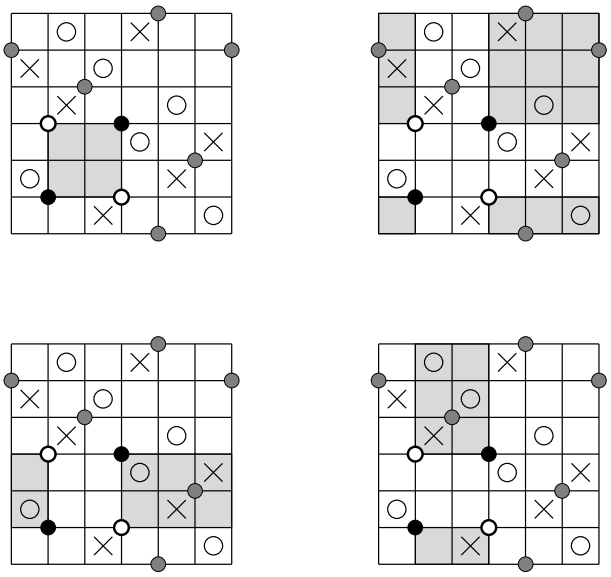

FIGURE 4.2. **Two grid states and the four rectangles connecting them.** Black dots appear in only one, call it $\mathbf{x}$; white dots appear in only the other one, call it $\mathbf{y}$; and gray dots appear in both. The two rectangles on the top row go from $\mathbf{x}$ to $\mathbf{y}$, and the other two go from $\mathbf{y}$ to $\mathbf{x}$. The top left rectangle is empty, and the other three are not.

For $\mathbf{x}, \mathbf{y} \in \mathbf{S}(\mathbb{G})$, let $\mathrm{Rect}(\mathbf{x}, \mathbf{y})$ denote the set of rectangles from $\mathbf{x}$ to $\mathbf{y}$. The set $\mathrm{Rect}(\mathbf{x}, \mathbf{y})$ is either empty, or it consists of exactly two rectangles, in which case $\mathrm{Rect}(\mathbf{y}, \mathbf{x})$ also consists of two rectangles. See Figure 4.2 for an illustration.

When we speak of a "rectangle", we will think of it as the geometric subset of the torus, together with the initial and the terminal grid states $\mathbf{x}$ and $\mathbf{y}$. Thus, if $\mathbf{x} \neq \mathbf{x}'$, a rectangle from $\mathbf{x}$ to $\mathbf{y}$ is always thought of as different from a rectangle from $\mathbf{x}'$ to $\mathbf{y}'$, even if their underlying polygons in the torus are the same. The underlying polygon is called the *support* of the rectangle.

Label the four corners of any rectangle as *northeast*, *southeast*, *northwest*, and *southwest*. This can be done, for example, by lifting r to the universal cover, which inherits a preferred pair of coordinates: the horizontal direction which is oriented eastward, and the vertical direction, which is oriented northward, following the conventions of Section 3.2. Sometimes we refer to the northwest corner as the upper left one, and the southeast corner as the lower right one.

If r is a rectangle from $\mathbf{x}$ to $\mathbf{y}$, then r contains elements of $\mathbf{x}$ and $\mathbf{y}$ on its boundary. The northeast and southwest corners of r are elements of $\mathbf{x}$, called *initial corners*, and the southeast and northwest corners of r are elements of $\mathbf{y}$, called *terminal corners*. The rectangle r might in addition contain elements of $\mathbf{x}$ in its interior $\mathrm{Int}(r)$. Note that $\mathbf{x} \cap \mathrm{Int}(r) = \mathbf{y} \cap \mathrm{Int}(r)$.

The following rectangles will play a special role in our subsequent constructions:

DEFINITION 4.2.1. A rectangle $r \in \mathrm{Rect}(\mathbf{x}, \mathbf{y})$ is called an ***empty rectangle*** if

$$\mathbf{x} \cap \mathrm{Int}(r) = \mathbf{y} \cap \mathrm{Int}(r) = \emptyset.$$

The set of empty rectangles from $\mathbf{x}$ to $\mathbf{y}$ is denoted $\mathrm{Rect}^\circ(\mathbf{x},\mathbf{y})$.

4.3. The bigrading on grid states

The grid complexes are equipped with two gradings called the *Maslov grading* and the *Alexander grading*, both induced by integral-valued functions on grid states for a toroidal grid diagram. The aim of this section is to construct these functions. Key properties of both functions are stated in the next two propositions, whose proofs will occupy the rest of the section. We start with the Maslov function.

PROPOSITION 4.3.1. *For any toroidal grid diagram $\mathbb{G}$, there is a function*

$$M_{\mathbb{O}}\colon \mathbf{S}(\mathbb{G}) \to \mathbb{Z},$$

called the ***Maslov function on grid states****, which is uniquely characterized by the following two properties:*

(M-1) Let $\mathbf{x}^{NWO}$ be the grid state whose components are the upper left corners of the squares marked with O. Then,

$$M_{\mathbb{O}}(\mathbf{x}^{NWO}) = 0. \tag{4.1}$$

(M-2) If $\mathbf{x}$ and $\mathbf{y}$ are two grid states that can be connected by some rectangle $r \in \mathrm{Rect}(\mathbf{x},\mathbf{y})$, then

$$M_{\mathbb{O}}(\mathbf{x}) - M_{\mathbb{O}}(\mathbf{y}) = 1 - 2\#(r \cap \mathbb{O}) + 2\#(\mathbf{x} \cap \mathrm{Int}(r)). \tag{4.2}$$

Note that $M_{\mathbb{O}}$ is independent of the placement of the X-markings. There is another function, $M_{\mathbb{X}}$ defined as in Proposition 4.3.1, only using the X-markings in place of the O-markings. Unless explicitly stated otherwise, the Maslov function on states refers to $M_{\mathbb{O}}$; and we will usually drop $\mathbb{O}$ from its notation.

DEFINITION 4.3.2. The ***Alexander function on grid states*** is defined in terms of the Maslov functions by the formula

$$A(\mathbf{x}) = \frac{1}{2}(M_{\mathbb{O}}(\mathbf{x}) - M_{\mathbb{X}}(\mathbf{x})) - \left(\frac{n-1}{2}\right). \tag{4.3}$$

Key properties of the Alexander function are captured in the following:

PROPOSITION 4.3.3. *Let $\mathbb{G}$ be a toroidal grid diagram for a knot. The function A is characterized, up to an overall additive constant, by the following property. For any rectangle $r \in \mathrm{Rect}(\mathbf{x},\mathbf{y})$ connecting two grid states $\mathbf{x}$ and $\mathbf{y}$,*

$$A(\mathbf{x}) - A(\mathbf{y}) = \#(r \cap \mathbb{X}) - \#(r \cap \mathbb{O}). \tag{4.4}$$

Furthermore, A is integral valued.

We prove Proposition 4.3.1 first. This is done by constructing a candidate function for $M_{\mathbb{O}}$, and verifying that it has the properties specified in Proposition 4.3.1. The candidate function is defined in terms of a planar realization of the toroidal grid, using the following construction.

DEFINITION 4.3.4. Consider the partial ordering on points in the plane $\mathbb{R}^2$ specified by $(p_1,p_2) < (q_1,q_2)$ if $p_1 < q_1$ and $p_2 < q_2$. If P and Q are sets of finitely many points in the plane, let $\mathcal{I}(P,Q)$ denote the number of pairs $p \in P$ and $q \in Q$ with $p < q$. We symmetrize this function, defining

$$\mathcal{J}(P,Q) = \frac{\mathcal{I}(P,Q) + \mathcal{I}(Q,P)}{2}.$$

Consider a fundamental domain $[0,n)\times[0,n)$ for the torus in the plane, with its left and bottom edges included. A grid state $\mathbf{x}\in\mathbf{S}(\mathbb{G})$ can be viewed as a collection of points with integer coordinates in this fundamental domain. Similarly, $\mathbb{O}=\{O_i\}_{i=1}^n$ can be viewed as a collection of points in the plane with half-integer coordinates in the fundamental domain.

During the course of our proof, we will find that $M_{\mathbb{O}}$ is given by the formula

$$M_{\mathbb{O}}(\mathbf{x})=\mathcal{J}(\mathbf{x},\mathbf{x})-2\mathcal{J}(\mathbf{x},\mathbb{O})+\mathcal{J}(\mathbb{O},\mathbb{O})+1, \tag{4.5}$$

which we write more succinctly as

$$M_{\mathbb{O}}(\mathbf{x})=\mathcal{J}(\mathbf{x}-\mathbb{O},\mathbf{x}-\mathbb{O})+1,$$

thinking of $\mathcal{J}$ as extended bilinearly over formal sums and formal differences of subsets of the plane. Correspondingly, $M_{\mathbb{X}}$ is given by

$$M_{\mathbb{X}}(\mathbf{x})=\mathcal{J}(\mathbf{x}-\mathbb{X},\mathbf{x}-\mathbb{X})+1.$$

LEMMA 4.3.5. *Fix a planar realization of a toroidal grid diagram. The function* $M(\mathbf{x})=\mathcal{J}(\mathbf{x}-\mathbb{O},\mathbf{x}-\mathbb{O})+1$ *satisfies Properties* (M-1) *and* (M-2).

Proof. Let $NW(O_i)$ denote the northwest corner of the square marked with O_i, and then project it to the fundamental domain. Clearly,

$$\begin{aligned} M(\mathbf{x}^{NWO}) =&\#\{(i,j)\big|NW(O_i)<NW(O_j)\}-\#\{(i,j)\big|NW(O_i)<O_j\}\\ &-\#\{(i,j)\big|O_i<NW(O_j)\}+\#\{(i,j)\big|O_i<O_j\}+1. \end{aligned} \tag{4.6}$$

To verify Equation (4.1), we count the number of times each pair (i,j) appears in the four sets on the right of Equation (4.6). We break this analysis into the following cases:

- If $i\neq j$ and neither O_i nor O_j is in the top row, then the following four inequalities are equivalent: $O_i<O_j$, $NW(O_i)<O_j$, $O_i<NW(O_j)$, and $NW(O_i)<NW(O_j)$.
- If O_j is in the top row and $i\neq j$, then $O_i<O_j$ is equivalent to $NW(O_i)<O_j$; while neither of $O_i<NW(O_j)$ nor $NW(O_i)<NW(O_j)$ can hold (since $NW(O_j)$ is in the bottom segment).
- If O_i is in the top row and $i\neq j$, neither $O_i<O_j$ nor $O_i<NW(O_j)$ can hold, while $NW(O_i)<O_j$ is equivalent to $NW(O_i)<NW(O_j)$.
- When $i=j$, there is exactly one O_i-marking for which $NW(O_i)<O_i$, when the O_i is in the top row. Note also that the three other inequalities $O_i<O_i$, $O_i<NW(O_i)$ and $NW(O_i)<NW(O_i)$ are never satisfied.

The total to the right-hand-side of Equation (4.6) from the first three cases are all 0, while the last case contributes -1. It follows that $M(\mathbf{x}^{NWO})=0$; i.e. M satisfies Property (M-1), as stated.

We verify that M satisfies Property (M-2), starting with the case where the rectangle r is contained in the fundamental domain for the torus used to define M. Label the southwest, northeast, northwest, and southeast corners of r by x_1, x_2, y_1, and y_2 respectively. Clearly,

$$\mathbf{x}=\{x_1,x_2\}\cup\mathbf{p} \text{ and } \mathbf{y}=\{y_1,y_2\}\cup\mathbf{p},$$

where $\mathbf{p} = \mathbf{x} \cap \mathbf{y}$. It is easy to see that

$$\begin{aligned}\mathcal{J}(\mathbf{x},\mathbf{x}) - \mathcal{J}(\mathbf{y},\mathbf{y}) &= 1 + \#\{x \in \mathbf{p} \big| x > x_1\} + \#\{x \in \mathbf{p} \big| x > x_2\} \\ &\quad + \#\{x \in \mathbf{p} \big| x < x_1\} + \#\{x \in \mathbf{p} \big| x < x_2\} - \#\{x \in \mathbf{p} \big| x > y_1\} \\ &\quad - \#\{x \in \mathbf{p} \big| x > y_2\} - \#\{x \in \mathbf{p} \big| x < y_1\} - \#\{x \in \mathbf{p} \big| x < y_2\} \\ &= 1 + 2\{x \in \mathbf{p} \big| x_1 < x < x_2\} = 1 + 2\#(\mathbf{x} \cap \mathrm{Int}(r)).\end{aligned}$$

Above, the contribution of 1 comes from the pair $x_1 < x_2$. Similarly,

$$\begin{aligned}2\mathcal{J}(\mathbf{x},\mathbb{O}) - 2\mathcal{J}(\mathbf{y},\mathbb{O}) &= \#\{O_i \in \mathbb{O} \big| O_i > x_1\} + \#\{O_i \in \mathbb{O} \big| O_i > x_2\} \\ &\quad + \#\{O_i \in \mathbb{O} \big| O_i < x_1\} + \#\{O_i \in \mathbb{O} \big| O_i < x_2\} - \#\{O_i \in \mathbb{O} \big| O_i > y_1\} \\ &\quad - \#\{O_i \in \mathbb{O} \big| O_i > y_2\} - \#\{O_i \in \mathbb{O} \big| O_i < y_1\} - \#\{O_i \in \mathbb{O} \big| O_i < y_2\} \\ &= 2\#\{O_i \in \mathbb{O} \big| x_1 < O_i < x_2\} = 2\#(\mathbb{O} \cap r).\end{aligned}$$

The above two equations imply that Equation (4.2) holds when r is contained in the fundamental domain used to define Equation (4.5).

Next suppose that r satisfies Equation (4.2). Suppose that $r' \in \mathrm{Rect}(\mathbf{y},\mathbf{x})$ is the rectangle with the property that r and r' meet along both horizontal edges, so that, in particular, both have the same width v. Then, since every column contains an O, and every vertical circle contains a component of $\mathbf{x}$, it follows that

$$\begin{aligned}\#(r' \cap \mathbb{O}) + \#(r \cap \mathbb{O}) &= v \\ \#(\mathbf{x} \cap \mathrm{Int}(r')) + \#(\mathbf{x} \cap \mathrm{Int}(r)) &= v - 1.\end{aligned}$$

These two equations, together with Equation (4.2) (for r), show that

$$M(\mathbf{y}) - M(\mathbf{x}) = 1 - 2\#(r' \cap \mathbb{O}) + 2\#(\mathbf{x} \cap \mathrm{Int}(r')),$$

which is the analogue of Equation (4.2) for r'.

In exactly the same manner, Equation (4.2) for r implies the same property for the rectangle that shares two vertical edges with r.

It follows that if Equation (4.2) holds for any rectangle $r \in \mathrm{Rect}(\mathbf{x},\mathbf{y})$, then the same holds for any other rectangle in $\mathrm{Rect}(\mathbf{x},\mathbf{y}) \cup \mathrm{Rect}(\mathbf{y},\mathbf{x})$. It is easy to see that at least one of the four rectangles in $\mathrm{Rect}(\mathbf{x},\mathbf{y}) \cup \mathrm{Rect}(\mathbf{y},\mathbf{x})$ is contained in the fundamental domain, for which we have already verified Equation (4.2); and hence the function defined in Equation (4.5) satisfies Property (M-2). □

Proof of Proposition 4.3.1. Lemma 4.3.5 verifies the existence of a function that satisfies Properties (M-1) and (M-2). To see that the function is uniquely characterized by these properties, observe that for any two grid states $\mathbf{x}$ and $\mathbf{y}$, there is a sequence of grid states $\mathbf{x} = \mathbf{x}_1, \mathbf{x}_2, \dots, \mathbf{x}_k = \mathbf{y}$ and rectangles $r_i \in \mathrm{Rect}(\mathbf{x}_i, \mathbf{x}_{i+1})$. This follows from the fact that the symmetric group is generated by transpositions. Thus the function $M(\mathbf{x})$ is uniquely determined up to an overall additive constant by Equation (4.2). Equation (4.1) specifies this constant. □

Note that Equation (4.5) specifies $M_{\mathbb{O}}$ using a fundamental domain; but the properties from Proposition 4.3.1 that uniquely characterize $M_{\mathbb{O}}$ make no reference to this choice. It follows that $M_{\mathbb{O}}$ is independent of the fundamental domain.

Next, we verify Equation (4.4), characterizing the Alexander function A.

Proof of Proposition 4.3.3. By Equation (4.2), if $r \in \mathrm{Rect}(\mathbf{x}, \mathbf{y})$ is any rectangle connecting the two grid states $\mathbf{x}$ and $\mathbf{y}$, then

$$M_{\mathbb{O}}(\mathbf{x}) - M_{\mathbb{O}}(\mathbf{y}) = 1 - 2\#(r \cap \mathbb{O}) + 2\#(\mathbf{x} \cap \mathrm{Int}(r))$$
$$M_{\mathbb{X}}(\mathbf{x}) - M_{\mathbb{X}}(\mathbf{y}) = 1 - 2\#(r \cap \mathbb{X}) + 2\#(\mathbf{x} \cap \mathrm{Int}(r))$$

Taking the difference of these two equations, and applying Equation (4.3), we conclude that Equation (4.4) holds. The function A is characterized up to an additive constant by Equation (4.4), since we can connect any two grid states by a sequence of rectangles.

The fact that M takes values in $\mathbb{Z}$ implies only that A takes values in $\frac{1}{2}\mathbb{Z}$. In view of Equation (4.4), to see that the Alexander function is integral, it suffices to show that there is one grid state $\mathbf{x}$ for which $A(\mathbf{x})$ is integral. Taking $\mathbf{x} = \mathbf{x}^{NWO}$, and using Equation (4.1), it suffices to show that

$$M_{\mathbb{X}}(\mathbf{x}^{NWO}) \equiv n - 1 \pmod 2. \tag{4.7}$$

To this end, we find a sequence of grid states $\mathbf{x}_i \in \mathbf{S}(\mathbb{G})$ for $i = 1, \dots, n$, with the following properties:

- $\mathbf{x}_1 = \mathbf{x}^{NWX}$ is the grid state whose components are the northwest corners of the squares marked with X,
- $\mathbf{x}_n = \mathbf{x}^{NWO}$,
- there is a (not necessarily empty) rectangle connecting $\mathbf{x}_i$ to $\mathbf{x}_{i+1}$.

This sequence can be found, since the permutation that connects $\mathbf{x}^{NWO}$ to $\mathbf{x}^{NWX}$ is a cycle of length n (since the grid represents a knot), and such a cycle can be written as a product of $n - 1$ transpositions. By Equation (4.1), $M_{\mathbb{X}}(\mathbf{x}_1) = 0$; so Equation (4.7) now follows from the mod 2 reduction of Equation (4.2). □

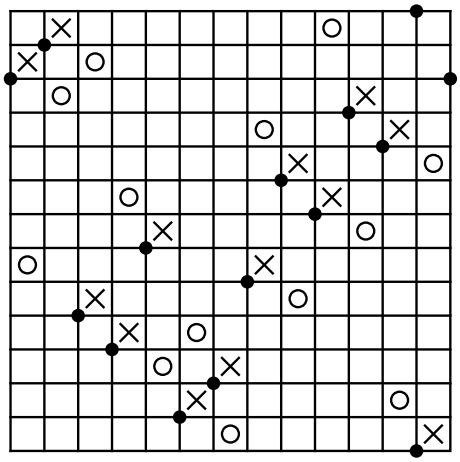

FIGURE 4.3. **Grid diagram for the 0-framed, negative Whitehead double of the left-handed trefoil knot.** The grid state $\mathbf{x}$ depicted in the diagram has Maslov grading 2.

EXERCISE 4.3.6. Consider the grid diagram $\mathbb{G}$ of Figure 4.3. Show that $\mathbb{G}$ represents $W_0^-(T_{-2,3})$, the 0-framed, negative Whitehead double of the left-handed

trefoil knot. Determine the Maslov and Alexander gradings of the grid state $\mathbf{x}$ indicated in the diagram. This example will play a crucial role in Section 8.6.

The following result will be useful later:

PROPOSITION 4.3.7. *Let $\mathbf{x}^{SWO}$ be the grid state whose components are the lower left (SW) corners of the squares marked with O. Then, $M(\mathbf{x}^{SWO}) = 1 - n$ for any $n \times n$ grid.*

Proof. Using the formula $M(\mathbf{x}^{SWO}) = \mathcal{J}(\mathbf{x}^{SWO} - \mathbb{O}, \mathbf{x}^{SWO} - \mathbb{O}) + 1$, we see that almost all terms cancel in pairs, except for the n pairs O_i and their corresponding $SW(O_i)$. The result follows. □

EXERCISE 4.3.8. Let $\mathbb{G}$ be any grid diagram, and let $\mathbf{x}^{SEO}$ and $\mathbf{x}^{NEO}$, respectively, be the grid state whose components are the lower resp. the upper right corners of the squares marked with O. Compute $M(\mathbf{x}^{SEO})$ and $M(\mathbf{x}^{NEO})$.

4.4. The simplest version of grid homology

In the various grid complexes studied in the present book, the boundary maps count certain empty rectangles. The various constructions differ in how the empty rectangles are counted, in terms of how they interact with the $\mathbb{X}$- and $\mathbb{O}$-markings. (Compare also Section 5.5, where a different construction is outlined.) The simplest version of the grid complex is the following:

DEFINITION 4.4.1. The ***fully blocked grid chain complex*** associated to the grid diagram $\mathbb{G}$ is the chain complex $\widetilde{GC}(\mathbb{G})$, whose underlying vector space over $\mathbb{F} = \mathbb{Z}/2\mathbb{Z}$ has a basis corresponding to the set of grid states $\mathbf{S}(\mathbb{G})$, and whose differential is specified by

$$\tilde{\partial}_{\mathbb{O},\mathbb{X}}(\mathbf{x}) = \sum_{\mathbf{y} \in \mathbf{S}(\mathbb{G})} \#\{r \in \mathrm{Rect}^{\circ}(\mathbf{x}, \mathbf{y}) \big| r \cap \mathbb{O} = r \cap \mathbb{X} = \emptyset\} \cdot \mathbf{y}. \tag{4.8}$$

Here $\#\{\cdot\}$ denotes the number of elements in the set modulo 2. (The subscript on $\tilde{\partial}_{\mathbb{O},\mathbb{X}}$ indicates the fact that the map counts rectangles that are disjoint from $\mathbb{O}$ and $\mathbb{X}$.)

The reader is invited to show that $\tilde{\partial}^2_{\mathbb{O},\mathbb{X}} = 0$. This is verified by interpreting the terms in $\tilde{\partial}^2_{\mathbb{O},\mathbb{X}}$ as counts of regions in the grid diagram that are compositions of two rectangles, and then showing that such regions have exactly two different decompositions into two rectangles, giving rise to pairwise cancelling terms in $\tilde{\partial}^2_{\mathbb{O},\mathbb{X}}$. A more general fact will be proved in Lemma 4.6.7 below.

The Maslov and Alexander functions on $\mathbf{S}(\mathbb{G})$ induce two gradings on $\widetilde{GC}(\mathbb{G})$: we define $\widetilde{GC}_d(\mathbb{G}, s)$ to be the $\mathbb{F}$-vector space generated by grid states $\mathbf{x}$ with $M(\mathbf{x}) = d$ and $A(\mathbf{x}) = s$. It follows quickly from Equations (4.2) and (4.4) that the restriction of $\tilde{\partial}_{\mathbb{O},\mathbb{X}}$ to $\widetilde{GC}_d(\mathbb{G}, s)$ maps into $\widetilde{GC}_{d-1}(\mathbb{G}, s)$. Thus, the bigrading descends to a bigrading on the homology groups of $\widetilde{GC}(\mathbb{G})$. Explicitly, letting

$$\widetilde{GH}_d(\mathbb{G}, s) = \frac{\mathrm{Ker}(\tilde{\partial}_{\mathbb{O},\mathbb{X}}) \cap \widetilde{GC}_d(\mathbb{G}, s)}{\mathrm{Im}(\tilde{\partial}_{\mathbb{O},\mathbb{X}}) \cap \widetilde{GC}_d(\mathbb{G}, s)},$$

then

$$\widetilde{GH}(\mathbb{G}) = \bigoplus_{d,s\in\mathbb{Z}} \widetilde{GH}_d(\mathbb{G}, s).$$

A *bigraded vector space* X is a vector space equipped with a splitting indexed by a pair of integers: $X = \bigoplus_{d,s\in\mathbb{Z}} X_{d,s}$. In this language, the Maslov and Alexander functions give $\widetilde{GH}(\mathbb{G})$ the structure of a bigraded vector space.

DEFINITION 4.4.2. The ***fully blocked grid homology*** of $\mathbb{G}$, denoted $\widetilde{GH}(\mathbb{G})$, is the homology of the chain complex $(\widetilde{GC}(\mathbb{G}), \tilde{\partial}_{\mathbb{O},\mathbb{X}})$, thought of as a bigraded vector space.

EXERCISE 4.4.3. Let $\mathcal{O}$ denote the unknot. Compute $\widetilde{GH}(\mathbb{G})$ for a 2×2 grid for $\mathcal{O}$. Compute $\widetilde{GH}(\mathbb{G})$ for a 3×3 grid for $\mathcal{O}$.

The above exercise demonstrates the fact that the total dimension of the homology $\widetilde{GH}(\mathbb{G})$ depends on the grid presentation of the knot. In fact, the following will be proved in Section 5.3:

THEOREM 4.4.4. *If $\mathbb{G}$ is a grid diagram with grid number n representing a knot K, then the renormalized dimension $\dim_{\mathbb{F}}(\widetilde{GH}(\mathbb{G}))/2^{n-1}$ is an integer-valued knot invariant; in particular, it is independent of the chosen grid presentation of K.*

4.5. Background on chain complexes

Theorem 4.4.4 might seem mysterious at this point. Indeed, even the fact that the dimension of $\widetilde{GH}(\mathbb{G})$ is divisible by 2^{n-1} is surprising. To verify this latter fact, it is helpful to enrich our coefficient ring to a polynomial algebra and to define a version of the grid complex over this algebra.

In the present section, we recall the necessary tools from homological algebra needed to study this enrichment. This material is essentially standard, with small modifications needed to accommodate the natural gradings arising in grid homology. More details, and proofs of some of these results, are provided in Appendix A.

Fix a commutative ring $\mathbb{K}$ with unit, which in our applications will be either $\mathbb{Z}$, the finite field $\mathbb{Z}/p\mathbb{Z}$ for some prime p, or $\mathbb{Q}$. In fact, through most of this text, we will take $\mathbb{K} = \mathbb{Z}/2\mathbb{Z} = \mathbb{F}$. Consider the polynomial ring $\mathcal{R} = \mathbb{K}[V_1, \dots, V_n]$ in n formal variables $V_1, \dots, V_n$. (We also allow $n = 0$, so that $\mathcal{R} = \mathbb{K}$.)

DEFINITION 4.5.1. A ***bigraded $\mathcal{R}$-module*** M is an $\mathcal{R}$-module, together with a splitting $M = \bigoplus_{d,s\in\mathbb{Z}} M_{d,s}$ as a $\mathbb{K}$-module, so that for each $i = 1, \dots, n$, V_i maps $M_{d,s}$ into $M_{d-2,s-1}$. A ***bigraded $\mathcal{R}$-module homomorphism*** is a homomorphism $f\colon M \to M'$ between two bigraded $\mathcal{R}$-modules that sends $M_{d,s}$ to $M'_{d,s}$ for all $d, s \in \mathbb{Z}$. More generally, an $\mathcal{R}$-module homomorphism from $f\colon M \to M'$ is said to be ***homogeneous of degree*** (m, t) if it sends $M_{d,s}$ to $M'_{d+m,s+t}$ for all $d, s \in \mathbb{Z}$.

A ***bigraded chain complex over*** $\mathcal{R} = \mathbb{K}[V_1, \dots, V_n]$ is a bigraded $\mathcal{R}$-module C, equipped with an $\mathcal{R}$-module homomorphism $\partial\colon C \to C$ with $\partial \circ \partial = 0$ that maps $C_{d,s}$ into $C_{d-1,s}$; in particular, ∂ is a homomorphism of $\mathcal{R}$-modules that is homogeneous of degree $(-1, 0)$.

The case where $n = 1$ will be of particular relevance to us. In this case, we write the algebra $\mathcal{R}$ simply as $\mathbb{K}[U]$. When $n = 0$ and $\mathbb{K} = \mathbb{F}$, the bigraded modules are bigraded vector spaces, the structures we encountered in Section 4.4.

DEFINITION 4.5.2. Let (C,∂) and (C',∂') be two bigraded chain complexes over $\mathcal{R}=\mathbb{K}[V_1,\dots,V_n]$. A ***chain map*** $f\colon (C,\partial)\to(C',\partial')$ is a homomorphism of $\mathcal{R}$-modules, satisfying the property that $\partial'\circ f = f\circ\partial$. The chain map f is called a ***bigraded chain map*** if it is also a bigraded homomorphism. More generally, a chain map is called ***homogeneous of degree*** (m,t) if the underlying homomorphism is bigraded of degree (m,t). An ***isomorphism*** of bigraded chain complexes is a bigraded chain map $f\colon (C,\partial)\to(C',\partial')$ for which there is another bigraded chain map $g\colon (C',\partial')\to(C,\partial)$ with $f\circ g=\mathrm{Id}_{C'}$ and $g\circ f=\mathrm{Id}_C$. If there is an isomorphism from (C,∂) to (C',∂'), we say that they are ***isomorphic bigraded chain complexes***, and write $(C,\partial)\cong(C',\partial')$.

A bigraded chain map $f\colon C\to C'$ between two bigraded chain complexes over $\mathcal{R}$ induces a well-defined bigraded map on homology, denoted $H(f)\colon H(C)\to H(C')$.

If (C,∂) and (C',∂') are bigraded chain complexes over $\mathcal{R}$, and $f\colon (C,\partial)\to(C',\partial')$ is a chain map, we can form the quotient complex $(C',\partial')/\mathrm{Im}(f)$, which is also a chain complex over $\mathcal{R}$. When f is homogeneous of degree (m,t), the quotient complex is also a bigraded chain complex of $\mathcal{R}$-modules.

For example, if (C,∂) is a bigraded chain complex over $\mathcal{R}=\mathbb{K}[V_1,\dots,V_n]$ with $n\geq 1$, then multiplication by V_i $i\in\{1,\dots,n\}$ is a chain map $V_i\colon (C,\partial)\to(C,\partial)$. In this case, the quotient complex is denoted $\frac{C}{V_i}$; or more suggestively $\frac{C}{V_i=0}$. This construction can be iterated; e.g. we can take the quotient of the chain complex by the map $V_j\colon \frac{C}{V_i}\to\frac{C}{V_i}$; the corresponding quotient will be denoted $\frac{C}{V_i=V_j=0}$.

A short exact sequence of chain complexes induces a long exact sequence on homology, according to the following:

LEMMA 4.5.3. *Let (C,∂), (C',∂'), and (C'',∂'') be three bigraded chain complexes over $\mathcal{R}=\mathbb{K}[V_1,\dots,V_n]$. Suppose that $f\colon C\to C'$ is a chain map which is homogeneous of degree (m,t), and $g\colon C'\to C''$ is a bigraded chain map, both of which fit into a short exact sequence*

$$0\longrightarrow C\xrightarrow{f} C'\xrightarrow{g} C''\longrightarrow 0.$$

Then, there is a homomorphism of $\mathcal{R}$-modules $\delta\colon H(C'')\to H(C)$ that is homogeneous of degree $(-m-1,-t)$, which fits into a long exact sequence

$$\cdots\longrightarrow H_{d-m,s-t}(C)\xrightarrow{H(f)} H_{d,s}(C')\xrightarrow{H(g)} H_{d,s}(C'')\xrightarrow{\delta} H_{d-m-1,s-t}(C)\longrightarrow\cdots$$

The proof of the above standard result is recalled in Appendix A; see Lemma A.2.1.

DEFINITION 4.5.4. Suppose that $f,g\colon (C,\partial)\to(C',\partial')$ are two bigraded chain maps between two bigraded chain complexes over $\mathcal{R}$. The maps f and g are said to be ***chain homotopic*** if there is an $\mathcal{R}$-module homomorphism $h\colon C\to C'$ that is homogeneous of degree $(1,0)$, and that satisfies the formula

$$f-g=\partial'\circ h+h\circ\partial. \tag{4.9}$$

In this case, h is called a ***chain homotopy from*** g ***to*** f. More generally, if $f,g\colon (C,\partial)\to(C',\partial')$ are two chain maps that are homogeneous of degree (m,t), they are called ***chain homotopic*** if there is a map $h\colon C\to C'$ that is an $\mathcal{R}$-module homomorphism homogeneous of degree $(m+1,t)$ and satisfies Equation (4.9).

It is easy to verify that chain homotopic maps induce the same map on homology.

DEFINITION 4.5.5. A chain map $f\colon C \to C'$ is a ***chain homotopy equivalence*** if there is a chain map $\phi\colon C' \to C$, called a ***chain homotopy inverse to*** f, with the property that $f \circ \phi$ and $\phi \circ f$ are both chain homotopic to the respective identity maps. If there is a chain homotopy equivalence from C to C', then C and C' are said to be ***chain homotopy equivalent*** complexes.

PROPOSITION 4.5.6. *Let C and C' be two bigraded chain complexes of $\mathcal{R} = \mathbb{K}[V_1, \dots, V_n]$-modules. A chain map $f\colon C \to C'$, homogeneous of degree (m,t), naturally induces a chain map $\overline{f}\colon \frac{C}{V_i} \to \frac{C}{V_i}$ that is also homogeneous of degree (m,t). Moreover, if g is another chain map that is homogeneous of degree (m,t), a chain homotopy h from f to g induces a chain homotopy $\overline{h}$ from $\overline{f}$ to $\overline{g}$.*

Proof. Any $\mathcal{R}$-module homomorphism $\phi\colon C \to C'$ induces an $\mathcal{R}$-module homomorphism $\overline{\phi}\colon \frac{C}{V_i} \to \frac{C'}{V_i}$. In this notation, the differential ∂ on C induces the differential $\overline{\partial}$ on $\frac{C}{V_i}$. Also, the chain maps f, g, and the chain homotopy h induce maps $\overline{f}$, $\overline{g}$, and $\overline{h}\colon \frac{C}{V_i} \to \frac{C'}{V_i}$. The relation $\overline{\partial}' \circ \overline{h} + \overline{h} \circ \overline{\partial} = \overline{f} - \overline{g}$ is a consequence of the relation $\partial' \circ h + h \circ \partial = f - g$. □

4.6. The grid chain complex GC^-

We now enrich the grid complex to a bigraded chain complex over the ring $\mathcal{R} = \mathbb{F}[V_1, \dots, V_n]$. Various specializations of this complex give rise to different versions of grid homology.

To define the enrichment, it is useful to enumerate the set $\mathbb{O} = \{O_i\}_{i=1}^n$. This puts the O-markings in one-to-one correspondence with the generators V_i of the polynomial algebra $\mathcal{R}$. Informally, the unblocked grid complex is the $\mathcal{R}$-module generated by grid states, equipped with a differential $\partial^-_{\mathbb{X}}$ counting empty rectangles that may cross the O- but not the X-markings. The *multiplicity* $O_i(r)$ of the rectangle r at the marking O_i is defined to be either 1 or 0, depending on whether or not r contains O_i. This multiplicity is recorded as the exponent of the formal variable V_i. More explicitly:

DEFINITION 4.6.1. The ***(unblocked) grid complex*** $GC^-(\mathbb{G})$ is the free module over $\mathcal{R}$ generated by $\mathbf{S}(\mathbb{G})$, equipped with the $\mathcal{R}$-module endomorphism whose value on any $\mathbf{x} \in \mathbf{S}(\mathbb{G})$ is given by

$$\partial^-_{\mathbb{X}}\mathbf{x} = \sum_{\mathbf{y}\in\mathbf{S}(\mathbb{G})} \sum_{\{r\in \mathrm{Rect}^\circ(\mathbf{x},\mathbf{y}) \,\big|\, r\cap\mathbb{X}=\emptyset\}} V_1^{O_1(r)} \cdots V_n^{O_n(r)} \cdot \mathbf{y}. \tag{4.10}$$

The elements $V_1^{k_1} \cdots V_n^{k_n} \cdot \mathbf{x}$ where $\mathbf{x} \in \mathbf{S}(\mathbb{G})$ and $k_1, \dots, k_n$ are arbitrary, non-negative integers form a basis for the $\mathbb{F}$-vector space $GC^-(\mathbb{G})$. Extend the Maslov and Alexander functions (Proposition 4.3.1 and Definition 4.3.2) to this basis by

$$M(V_1^{k_1} \dots V_n^{k_n} \cdot \mathbf{x}) = M(\mathbf{x}) - 2k_1 - \cdots - 2k_n, \tag{4.11}$$

$$A(V_1^{k_1} \dots V_n^{k_n} \cdot \mathbf{x}) = A(\mathbf{x}) - k_1 - \cdots - k_n. \tag{4.12}$$

These extensions equip $GC^-(\mathbb{G})$ with a bigrading: let $GC^-_d(\mathbb{G}, s)$ denote the vector subspace spanned by basis vectors $V_1^{k_1} \cdots V_n^{k_n} \cdot \mathbf{x}$ with $M(V_1^{k_1} \cdots V_n^{k_n} \cdot \mathbf{x}) = d$, and $A(V_1^{k_1} \cdots V_n^{k_n} \cdot \mathbf{x}) = s$. If $x \in GC^-(\mathbb{G})$ lies in some $GC^-_d(\mathbb{G}, s)$ for some d and s, we say that x is *homogeneous with bigrading* (d, s) or simply *homogeneous*. (Note that the element 0 is homogeneous with any bigrading.)

REMARK 4.6.2. In Chapter 13, we will study another variant of the grid complex, $\mathcal{GC}^-(\mathbb{G})$, which has the same underlying $\mathcal{R}$-module as $GC^-(\mathbb{G})$, a grading induced by M, and a differential specified by

$$\partial^- \mathbf{x} = \sum_{\mathbf{y} \in \mathbf{S}(\mathbb{G})} \sum_{r \in \mathrm{Rect}^\circ(\mathbf{x}, \mathbf{y})} V_1^{O_1(r)} \cdots V_n^{O_n(r)} \cdot \mathbf{y}. \tag{4.13}$$

This complex has a filtration which is a knot invariant, and its total homology is isomorphic to $\mathbb{F}[U]$. The normalization of M specified by Equation (4.1) was chosen so that the generator of this homology module has grading equal to zero.

THEOREM 4.6.3. *The object* $(GC^-(\mathbb{G}), \partial^-_{\mathbb{X}})$ *is a bigraded chain complex over the ring* $\mathbb{F}[V_1, \dots, V_n]$*, in the sense of Definition* 4.5.1.

We break the proof of Theorem 4.6.3 into pieces, starting with the verification that $\partial^-_{\mathbb{X}} \circ \partial^-_{\mathbb{X}} = 0$. To this end, it is convenient to generalize the notion of rectangles.

Recall that the circles $\alpha_1, \dots, \alpha_g, \beta_1, \dots, \beta_g$ divide the torus into oriented squares $S_1, \dots, S_{n^2}$. A formal linear combination of the closures of these squares, $\mathcal{D} = \sum a_i \cdot \overline{S_i}$ with $a_i \in \mathbb{Z}$, has a boundary, which is a formal linear combination of intervals contained inside $\alpha_1 \cup \cdots \cup \alpha_n \cup \beta_1 \cup \cdots \cup \beta_n$. Let $\partial_\alpha \mathcal{D}$ be the portion of the boundary contained in $\alpha_1 \cup \cdots \cup \alpha_n$ and $\partial_\beta \mathcal{D}$ be the portion in $\beta_1 \cup \cdots \cup \beta_n$.

DEFINITION 4.6.4. Fix $\mathbf{x}, \mathbf{y} \in \mathbf{S}(\mathbb{G})$. A ***domain*** ψ from $\mathbf{x}$ to $\mathbf{y}$ is a formal linear combination of the closures of the squares in $\mathbb{G} \setminus (\boldsymbol{\alpha} \cup \boldsymbol{\beta})$, with the property that $\partial(\partial_\alpha \psi) = \mathbf{y} - \mathbf{x}$ and hence $\partial(\partial_\beta \psi) = \mathbf{x} - \mathbf{y}$. In these equations, the two sides represent a formal linear combinations of points; e.g. if $\mathbf{x} = \{x_1, \dots, x_n\}$ and $\mathbf{y} = \{y_1, \dots, y_n\}$, then $\mathbf{x} - \mathbf{y} = \sum_{i=1}^n (x_i - y_i)$. Denote the set of domains from $\mathbf{x}$ to $\mathbf{y}$ by $\pi(\mathbf{x}, \mathbf{y})$. A domain ψ is called ***positive*** if each square in the torus (with its orientation inherited from the torus) appears in the expression for ψ with non-negative multiplicity.

REMARK 4.6.5. The grid diagram $\mathbb{G}$ equips the torus with a CW-decomposition, whose 0-cells are the n^2 intersection points of the horizontal and the vertical circles; its 1-cells are the $2n^2$ intervals on the horizontal and vertical circles between consecutive intersections of these circles, and its 2-cells are the n^2 small squares of the grid diagram. A formal sum ψ of rectangles is a 2-chain in this CW-complex structure. The group of 1-chains splits as the sum of the span of the horizontal intervals and vertical intervals. The 1-chain $\partial_\alpha \psi$ is the part of $\partial \psi$ in the span of the horizontal intervals, so the relation $\partial(\partial_\alpha \psi) = \mathbf{y} - \mathbf{x}$ is an equation of 0-chains.

Domains can be composed: if $\phi \in \pi(\mathbf{x}, \mathbf{y})$ and $\psi \in \pi(\mathbf{y}, \mathbf{z})$, then by adding the two underlying 2-chains we get a new domain, written $\phi * \psi \in \pi(\mathbf{x}, \mathbf{z})$.

EXERCISE 4.6.6. **(a)** Show that any two $\mathbf{x}, \mathbf{y} \in \mathbf{S}(\mathbb{G})$ can be connected by a domain $\psi \in \pi(\mathbf{x}, \mathbf{y})$.
(b) Show that any two $\mathbf{x}, \mathbf{y} \in \mathbf{S}(\mathbb{G})$ can be connected by a domain $\psi \in \pi(\mathbf{x}, \mathbf{y})$ with $\mathbb{X} \cap \psi = \emptyset$.

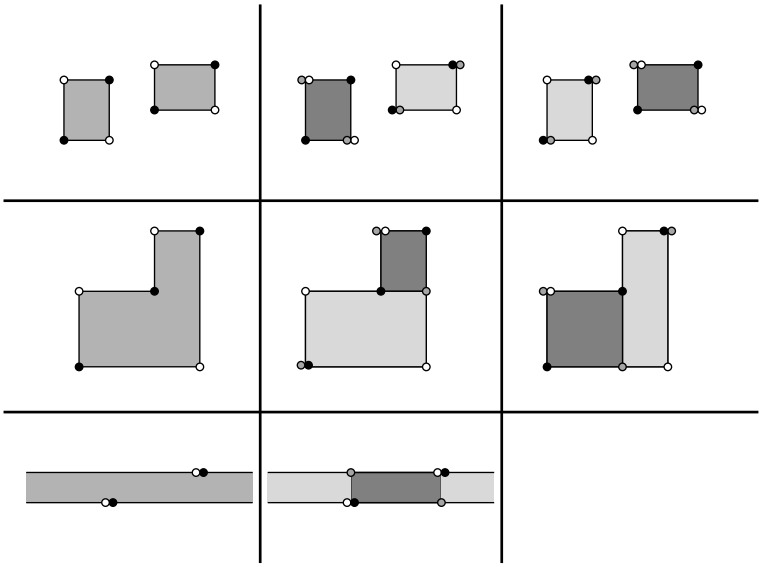

FIGURE 4.4. **Cases in the proof of Lemma 4.6.7.** The left column illustrates the three basic types of domains ψ with $N(\psi) > 0$ (Cases (R-1), (R-2), and (R-3), respectively). The initial grid state is indicated by black dots; the terminal one by the white dots. The second and third columns show the decompositions of the domain in the first column. The first rectangle in the decomposition is darker than the second. The intermediate grid state is indicated by gray dots. In the first row we consider the case of two disjoint rectangles; these rectangles can also overlap as in Figure 4.5.

(c) If $\mathbb{G}$ represents a knot, show that any domain $\psi \in \pi(\mathbf{x}, \mathbf{y})$ with $\mathbb{X} \cap \psi = \emptyset$ is uniquely determined by its multiplicities at the $\mathbb{O}$. What if $\mathbb{G}$ represents a link?

The next lemma will be used to establish Theorem 4.6.3. Its proof will serve as a prototype for many of the proofs from Chapter 5.

LEMMA 4.6.7. *The operator* $\partial^-_{\mathbb{X}} \colon GC^-(\mathbb{G}) \to GC^-(\mathbb{G})$ *satisfies* $\partial^-_{\mathbb{X}} \circ \partial^-_{\mathbb{X}} = 0$.

Proof. For grid states $\mathbf{x}$ and $\mathbf{z}$ fix $\psi \in \pi(\mathbf{x}, \mathbf{z})$ and (for the purposes of this proof) let $N(\psi)$ denote the number of ways we can decompose ψ as a composite of two empty rectangles $r_1 * r_2$. Observe that if $\psi = r_1 * r_2$ for some $r_1 \in \mathrm{Rect}(\mathbf{x}, \mathbf{y})$ and $r_2 \in \mathrm{Rect}(\mathbf{y}, \mathbf{z})$, the following statements hold:

- $\psi \cap \mathbb{X}$ is empty if and only if $r_i \cap \mathbb{X}$ is empty for both $i = 1, 2$.
- The local multiplicities of ψ, r_1, and r_2 at any $O_i \in \mathbb{O}$ are related by
$$O_i(\psi) = O_i(r_1) + O_i(r_2).$$

It follows that for any $\mathbf{x} \in \mathbf{S}(\mathbb{G})$,

$$\partial^-_{\mathbb{X}} \circ \partial^-_{\mathbb{X}}(\mathbf{x}) = \sum_{\mathbf{z} \in \mathbf{S}(\mathbb{G})} \sum_{\left\{\psi \in \pi(\mathbf{x}, \mathbf{z}) \,|\, \psi \cap \mathbb{X} = \emptyset\right\}} N(\psi) \cdot V_1^{O_1(\psi)} \cdots V_n^{O_n(\psi)} \cdot \mathbf{z}.$$

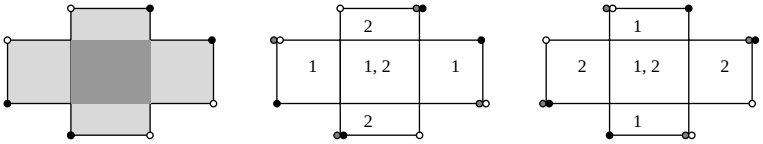

FIGURE 4.5. **Overlapping domains counted in $\partial^-_{\mathbb{X}} \circ \partial^-_{\mathbb{X}} = 0$.** Part of the domain on the left has local multiplicity two (indicated by the darker shading). The next two pictures show the two decompositions of this domain as a juxtaposition of two rectangles. The rectangles are labeled by integers 1 and 2, indicating their order in the decomposition.

Consider a pair of empty rectangles $r_1 \in \mathrm{Rect}^\circ(\mathbf{x}, \mathbf{y})$ and $r_2 \in \mathrm{Rect}^\circ(\mathbf{y}, \mathbf{z})$, so that $r_1 * r_2 = \psi$ is a domain with $N(\psi) > 0$. There are three basic cases (see also Figure 4.4 for an illustration):

(R-1) $\mathbf{x} \setminus (\mathbf{x} \cap \mathbf{z})$ consists of 4 elements. In this case, the corners of r_1 and r_2 are all distinct. There is a unique $\mathbf{y}' \in \mathbf{S}(\mathbb{G})$ and rectangles $r_1' \in \mathrm{Rect}^\circ(\mathbf{x}, \mathbf{y}')$ and $r_2' \in \mathrm{Rect}^\circ(\mathbf{y}', \mathbf{z})$ so that r_1 and r_2' have the same support and r_2 and r_1' have the same support. See the top row of Figure 4.4 (and also Figure 4.5). Then, $r_1 * r_2 = r_1' * r_2'$ and in fact $N(\psi) = 2$.

(R-2) $\mathbf{x} \setminus (\mathbf{x} \cap \mathbf{z})$ consists of 3 elements. In this case, the local multiplicities of ψ are all 0 or 1 and the corresponding region in the torus has six corners, five of which are $90°$, and one of which is $270°$. Cutting at the $270°$ corner in two different directions gives the two decompositions of ψ as a juxtaposition of empty rectangles $\psi = r_1 * r_2 = r_1' * r_2'$, where $r_1 \in \pi(\mathbf{x}, \mathbf{y})$, $r_2 \in \pi(\mathbf{y}, \mathbf{z})$, $r_1' \in \pi(\mathbf{x}, \mathbf{y}')$, and $r_2' \in \pi(\mathbf{y}', \mathbf{z})$ (with $\mathbf{y} \neq \mathbf{y}'$). In particular, $N(\psi) = 2$ in this case, as well. See the middle row of Figure 4.4.

(R-3) $\mathbf{x} = \mathbf{z}$. In this case, $\psi = r_1 * r_2$, where r_1 and r_2 intersect along two edges and therefore ψ is an annulus. Since r_1 and r_2 are empty, this annulus has height or width equal to 1. Such an annulus is called a *thin annulus*; see the bottom row of Figure 4.4. Thin annuli have $N(\psi) = 1$.

Contributions from Cases (R-1) and (R-2) cancel in pairs, since we are working modulo 2. There are no contributions from Case (R-3), since every thin annulus contains one X-marking in it, concluding the proof of the lemma. □

LEMMA 4.6.8. *The differential $\partial^-_{\mathbb{X}}$ is homogeneous of degree $(-1, 0)$.*

Proof. If $V_1^{k_1} \cdots V_n^{k_n} \cdot \mathbf{y}$ appears in $\partial^-_{\mathbb{X}} \mathbf{x}$, then there is a rectangle $r \in \mathrm{Rect}^\circ(\mathbf{x}, \mathbf{y})$ with $r \cap \mathbb{X} = \emptyset$, and $O_i(r) = k_i$ for $i = 1, \ldots, n$. By Equations (4.2) and (4.11),

$$M(V_1^{k_1} \cdots V_n^{k_n} \cdot \mathbf{y}) = M(\mathbf{y}) - 2\#(r \cap \mathbb{O}) = M(\mathbf{x}) - 1,$$

so the Maslov grading drops by one under the differential. Similarly, Equations (4.4) and (4.12) give

$$A(V_1^{k_1} \cdots V_n^{k_n} \cdot \mathbf{y}) = A(\mathbf{y}) - \#(r \cap \mathbb{O}) = A(\mathbf{x}) - \#(r \cap \mathbb{X}). \tag{4.14}$$

Since $r \cap \mathbb{X} = \emptyset$, it follows that $A(V_1^{k_1} \cdots V_n^{k_n} \cdot \mathbf{y}) = A(\mathbf{x})$; i.e. $\partial^-_{\mathbb{X}}$ preserves the Alexander grading. □

Proof of Theorem 4.6.3. Equations (4.11) and (4.12) ensure that multiplication by V_i is a homogeneous map of degree $(-2,-1)$; i.e. $GC^-(\mathbb{G})$ is a bigraded module over $\mathbb{F}[V_1,\dots,V_n]$. The differential is defined to be an $\mathcal{R}$-module homomorphism; Lemma 4.6.8 ensures that it is homogeneous of degree $(-1,0)$. The theorem now follows from Lemma 4.6.7. □

The complex $GC^-(\mathbb{G})$ generalizes $\widetilde{GC}(\mathbb{G})$, since

$$\frac{GC^-(\mathbb{G})}{V_1=\ldots=V_n=0}\cong\widetilde{GC}(\mathbb{G}). \tag{4.15}$$

We study now further properties of $GC^-(\mathbb{G})$.

LEMMA 4.6.9. *For any pair of integers $i,j\in\{1,\dots,n\}$ multiplication by V_i is chain homotopic to multiplication by V_j, when thought of as homogeneous maps from $GC^-(\mathbb{G})$ to itself of degree $(-2,-1)$.*

Proof. Variables V_i and V_j are called *consecutive* if there is a square marked by X in the same row as O_i and in the same column as O_j. Suppose that V_i and V_j are consecutive, and let X_i denote the X-marking in the same row as O_i and in the same column as O_j. Define a corresponding homotopy operator that counts rectangles that contain X_i in their interior:

$$\mathcal{H}_i(\mathbf{x})=\mathcal{H}_{X_i}(\mathbf{x})=\sum_{\mathbf{y}\in\mathbf{S}(\mathbb{G})}\sum_{\{r\in\mathrm{Rect}^\circ(\mathbf{x},\mathbf{y})\,\big|\,\mathrm{Int}(r)\cap\mathbb{X}=X_i\}}V_1^{O_1(r)}\cdots V_n^{O_n(r)}\cdot\mathbf{y}. \tag{4.16}$$

It follows immediately from Proposition 4.3.1 and Equation (4.4) that $\mathcal{H}_i$ is homogeneous of degree $(-1,-1)$. The proof of Lemma 4.6.7 shows that [1]

$$\partial^-_{\mathbb{X}}\circ\mathcal{H}_i+\mathcal{H}_i\circ\partial^-_{\mathbb{X}}=V_i-V_j.$$

In this adaptation, count decompositions of domains ψ with $N(\psi)>0$ and which contain X_i (and no other $X\in\mathbb{X}$) with multiplicity one in their interior. In addition to the types of pairs appearing in Cases (R-1) and (R-2) of Lemma 4.6.7, there are two thin annuli that contribute to $\partial^-_{\mathbb{X}}\circ\mathcal{H}_i+\mathcal{H}_i\circ\partial^-_{\mathbb{X}}$, and those are the two annuli (horizontal and vertical) through X_i. The contributions of these two annuli are multiplication by V_i and multiplication by V_j.

For general V_i and V_j, since K is a knot there is a sequence of variables $V_i=V_{n_1},\dots,V_{n_m}=V_j$ where V_{n_k} and $V_{n_{k+1}}$ are consecutive. Adding the chain homotopies, we deduce that V_i is homotopic to V_j. □

REMARK 4.6.10. Lemma 4.6.9 uses the fact that the grid diagram $\mathbb{G}$ represents a knot, rather than a link: in general, the actions of variables corresponding to different link components are not chain homotopic; cf. also Lemma 8.2.3. For more on the case of links, see Section 9.1 and Chapter 11.

DEFINITION 4.6.11. Fix some $i\in\{1,\dots,n\}$. The ***unblocked grid homology of*** $\mathbb{G}$, denoted $GH^-(\mathbb{G})$, is the homology of $(GC^-(\mathbb{G}),\partial^-_{\mathbb{X}})$, viewed as a bigraded module over $\mathbb{F}[U]$, where the action of U is induced by multiplication by V_i.

[1] Note that $V_i-V_j=V_i+V_j$ in $\mathcal{R}$. We write V_i-V_j, since that expression is what shows up when we work with $\mathbb{Z}$ coefficients, as in Chapter 15.

Lemma 4.6.9 shows that the grid homology groups, thought of as bigraded modules over $\mathbb{F}[U]$, are independent of the choice of i. Lemma 4.6.9 also inspires the following further construction:

DEFINITION 4.6.12. Fix some $i = 1, \dots, n$. The quotient complex $GC^-(\mathbb{G})/V_i$ is called the ***simply blocked grid complex***, and it is denoted $\widehat{GC}(\mathbb{G})$. The ***simply blocked grid homology of*** $\mathbb{G}$, $\widehat{GH}(\mathbb{G})$, is the bigraded vector space obtained as the homology of $\widehat{GC}(\mathbb{G}) = (GC^-(\mathbb{G})/V_i, \partial^-_{\mathbb{X}})$.

REMARK 4.6.13. Explicitly, $GC^-(\mathbb{G})/V_n$ is the bigraded $\mathbb{F}$-vector space with basis $V_1^{k_1} \cdots V_{n-1}^{k_{n-1}} \cdot \mathbf{x}$, where $k_1, \dots, k_{n-1}$ are arbitrary non-negative integers and $\mathbf{x} \in \mathbf{S}(\mathbb{G})$; equipped with a differential $\widehat{\partial}_{\mathbb{X},O_n}$ specified by $\widehat{\partial}_{\mathbb{X},O_n} \circ V_j = V_j \circ \widehat{\partial}_{\mathbb{X},O_n}$ for $j = 1, \dots, n-1$, and for any $\mathbf{x} \in \mathbf{S}(\mathbb{G})$,

$$\widehat{\partial}_{\mathbb{X},O_n}(\mathbf{x}) = \sum_{\mathbf{y} \in \mathbf{S}(\mathbb{G})} \sum_{\{r \in \mathrm{Rect}^\circ(\mathbf{x},\mathbf{y}) \,\big|\, r \cap \mathbb{X} = \emptyset, O_n(r) = 0\}} V_1^{O_1(r)} \cdots V_{n-1}^{O_{n-1}(r)} \cdot \mathbf{y}.$$

We shall see that $\widehat{GH}$ is a finite dimensional vector space that is independent of the choice of i, in Corollaries 4.6.16 and 4.6.17 below. But first, we explain how to extract the vector space $\widehat{GH}(\mathbb{G})$ from $\widehat{GH}(\mathbb{G})$, in terms of the following notation. Let X and Y be two bigraded vector spaces

$$X = \bigoplus_{d,s \in \mathbb{Z}} X_{d,s} \qquad \text{and} \qquad Y = \bigoplus_{d,s \in \mathbb{Z}} Y_{d,s}.$$

Their tensor product $X \otimes Y = \bigoplus_{d,s \in \mathbb{Z}} (X \otimes Y)_{d,s}$ is the bigraded vector space, with

$$(X \otimes Y)_{d,s} = \bigoplus_{\substack{d_1 + d_2 = d \\ s_1 + s_2 = s}} X_{d_1,s_1} \otimes Y_{d_2,s_2}. \tag{4.17}$$

DEFINITION 4.6.14. Let X be a bigraded vector space, and fix integers a and b. The corresponding ***shift of*** X, denoted $X[\![a,b]\!]$, is the bigraded vector space that is isomorphic to X as a vector space and given the bigrading $X[\![a,b]\!]_{d,s} = X_{d+a,s+b}$.

Let W be the two-dimensional bigraded vector space with one generator in bigrading $(0,0)$ and another in bigrading $(-1,-1)$, and let X be any other bigraded vector space, then the tensor product $X \otimes W$ is identified with two copies of X, one of which is equipped with a shift in degree:

$$X \otimes W \cong X \oplus X[\![1,1]\!]. \tag{4.18}$$

This can be iterated; for example, $X \otimes W^{\otimes 2} \cong X \oplus X[\![1,1]\!] \oplus X[\![1,1]\!] \oplus X[\![2,2]\!]$.

PROPOSITION 4.6.15. *Let $\mathbb{G}$ be a grid diagram representing a knot. Let W be the two-dimensional bigraded vector space, with one generator in bigrading $(0,0)$ and the other in bigrading $(-1,-1)$. Then, there is an isomorphism*

$$\widehat{GH}(\mathbb{G}) \cong \widehat{GH}(\mathbb{G}) \otimes W^{\otimes(n-1)} \tag{4.19}$$

of bigraded vector spaces, where $\widehat{GH}(\mathbb{G}) = H(\frac{GC^-(\mathbb{G})}{V_i})$ for any $i = 1, \dots, n$.

Proof. We will prove by induction on j that

$$H\left(\frac{GC^-(\mathbb{G})}{V_1 = \cdots = V_j = 0}\right) \cong H\left(\frac{GC^-(\mathbb{G})}{V_1 = 0}\right) \otimes W^{\otimes(j-1)}. \tag{4.20}$$

We interpret W^0 as a one-dimensional vector space in bigrading $(0,0)$, so that the isomorphism $W^{\otimes a}\otimes W\cong W^{\otimes(a+1)}$ holds for all $a\geq 0$. In the basic case where $j=1$, Equation (4.20) is a tautology.

For the inductive step, for $j>1$ consider the short exact sequence

(4.21)
$$0\longrightarrow \frac{GC^-(\mathbb{G})}{V_1=\cdots=V_{j-1}=0}\xrightarrow{V_j}\frac{GC^-(\mathbb{G})}{V_1=\cdots=V_{j-1}=0}\longrightarrow\frac{GC^-(\mathbb{G})}{V_1=\cdots=V_j=0}\longrightarrow 0.$$

Using Proposition 4.5.6, the chain homotopy between V_j and V_1 provided by Lemma 4.6.9, induces a chain homotopy between the chain map

$$V_j\colon \frac{GC^-(\mathbb{G})}{V_1=\cdots=V_{j-1}=0}\to\frac{GC^-(\mathbb{G})}{V_1=\cdots=V_{j-1}=0}$$

and the 0 map, so the long exact sequence on homology associated to the short exact squence from Equation (4.21) (cf. Lemma 4.5.3) becomes a short exact sequence

$$0\longrightarrow H\left(\frac{GC^-(\mathbb{G})}{V_1=\cdots=V_{j-1}=0}\right)\longrightarrow H\left(\frac{GC^-(\mathbb{G})}{V_1=\cdots=V_j=0}\right)\longrightarrow H\left(\frac{GC^-(\mathbb{G})}{V_1=\cdots=V_{j-1}=0}\right)\longrightarrow 0,$$

where the second arrow preserves bigradings, and the third is homogeneous of degree $(1,1)$. Thus, this short exact sequence of vector spaces translates into the first isomorphism of bigraded vector spaces appearing in the following:

$$H\left(\frac{GC^-(\mathbb{G})}{V_1=\cdots=V_j=0}\right)\cong H\left(\frac{GC^-(\mathbb{G})}{V_1=\cdots=V_{j-1}=0}\right)\otimes W\cong\widehat{GH}(\mathbb{G})\otimes W^{\otimes(j-1)},$$

and the second isomorphism follows from the inductive hypothesis. This completes the inductive step, verifying Equation (4.20) for all $j=1,\dots,n$.

In view of Equation (4.15), when $j=n$, Equation (4.20) gives Equation (4.19) for $i=1$. Numbering our formal variables differently, we conclude that Equation (4.19) holds for arbitrary i. □

The chain complex $\widetilde{GC}(\mathbb{G})$ is finite dimensional over $\mathbb{F}$, so its homology $\widetilde{GH}(\mathbb{G})$ is also finite dimensional. Although $\widehat{GC}(\mathbb{G})$ is infinite dimensional over $\mathbb{F}$, Proposition 4.6.15 has the following immediate consequence:

Corollary 4.6.16. *For a grid diagram $\mathbb{G}$ with grid number n, the vector space $\widehat{GH}(\mathbb{G})$ is finite dimensional, the dimension of $\widehat{GH}(\mathbb{G})$ is divisible by 2^{n-1}, and in fact $2^{n-1}\cdot\dim_{\mathbb{F}}\widehat{GH}(\mathbb{G})=\dim_{\mathbb{F}}\widetilde{GH}(\mathbb{G})$.* □

Corollary 4.6.17. *The simply blocked grid homology*

$$\widehat{GH}(\mathbb{G})=H(GC^-(\mathbb{G})/V_i)$$

is independent of the choice of $i=1,\dots,n$.

Proof. From Proposition 4.6.15, it follows that for i,j,

$$H\left(\frac{GC^-(\mathbb{G})}{V_i}\right)\otimes W^{(n-1)}\cong H\left(\frac{GC^-(\mathbb{G})}{V_j}\right)\otimes W^{(n-1)} \tag{4.22}$$

as bigraded vector spaces.

Just as a finite dimensional vector space is determined up to isomorphism by its dimension, a finite dimensional bigraded vector space Y is determined up to isomorphism by its *Poincaré polynomial* P_Y, the Laurent polynomial in q and t:

$$P_Y(q,t) = \sum_{d,s\in\mathbb{Z}} \dim Y_{d,s} \cdot q^d t^s. \tag{4.23}$$

Letting $Y_i = H(\frac{GC^-(\mathbb{G}))}{V_i})$, Equation (4.22) translates into the equation

$$(1+q^{-1}t^{-1})^{n-1} \cdot P_{Y_i}(q,t) = (1+q^{-1}t^{-1})^{n-1} \cdot P_{Y_j}(q,t),$$

so $P_{Y_i} = P_{Y_j}$, and hence $H(\frac{GC^-(\mathbb{G})}{V_i}) \cong H(\frac{GC^-(\mathbb{G})}{V_j})$ as bigraded vector spaces. □

Another relation among the grid homology groups is given by the following:

PROPOSITION 4.6.18. *There is a long exact sequence relating* $\widehat{GH}(\mathbb{G})$ *and* $GH^-(\mathbb{G})$*:*

$$\cdots \to GH^-_{d+2}(\mathbb{G}, s+1) \xrightarrow{U} GH^-_d(\mathbb{G}, s) \to \widehat{GH}_d(\mathbb{G}, s) \to GH^-_{d+1}(\mathbb{G}, s+1) \to \dots$$

Proof. Consider the short exact sequence

$$0 \to GC^-(\mathbb{G}) \xrightarrow{V_i} GC^-(\mathbb{G}) \to \widehat{GC}(\mathbb{G}) \to 0$$

of bigraded chain complexes of $\mathbb{F}[V_i]$-modules, where the first map is, of course, homogeneous of degree $(-2,-1)$. The associated long exact sequence in homology (Lemma 4.5.3) gives the statement of the proposition. □

A key feature of the grid homology groups $\widehat{GH}(\mathbb{G})$ and $GH^-(\mathbb{G})$ is that they are knot invariants, in the following sense.

THEOREM 4.6.19. *The homologies* $\widehat{GH}(\mathbb{G})$ *and* $GH^-(\mathbb{G})$ *(the former thought of as a bigraded* $\mathbb{F}$*-vector space, the latter thought of as a bigraded* $\mathbb{F}[U]$*-module) depend on the grid* $\mathbb{G}$ *only through its underlying (unoriented) knot* K*.*

The proof of the above theorem will be given in Chapter 5.

4.7. The Alexander grading as a winding number

The aim of the present section is to give geometric insight into the bigrading from Section 4.3. Byproducts include a practical formula for computing A and a relationship between grid homology and the Alexander polynomial. The geometric interpretation of the Alexander grading rests on the following formula, which expresses the winding number about a knot projection in terms of planar grid diagrams.

LEMMA 4.7.1. *Let* $\mathbb{G}$ *be a planar grid diagram of a knot* K*, let* $\mathcal{D} = \mathcal{D}(\mathbb{G})$ *be the corresponding knot projection in the plane, and let* p *be any point not on* $\mathcal{D}$*. Then, the winding number* $w_{\mathcal{D}}(p)$ *of* $\mathcal{D}$ *around* p *is computed by the formula*

$$w_{\mathcal{D}}(p) = \mathcal{J}(p, \mathbb{O} - \mathbb{X}). \tag{4.24}$$

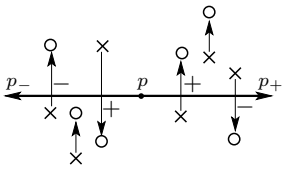

FIGURE 4.6. **Winding numbers**. The diagram illustrates the equality $w_{\mathcal{D}}(p) = \mathcal{I}(p, \mathbb{O} - \mathbb{X})$ (interpreting the winding number as intersection of the knot projection with the ray p_+), and at the same time the equality $w_{\mathcal{D}}(p) = \mathcal{I}(\mathbb{O} - \mathbb{X}, p)$ (interpreting the winding number as intersection with the ray p_-).

Proof. If $p = (x, y)$ is any point not contained in $\mathcal{D}$, then $\mathcal{I}(p, \mathbb{O} - \mathbb{X})$ is the (signed) intersection number of the ray p_+ from p to $(+\infty, y)$ with $\mathcal{D}$: the vertical arc connecting some O with X contributes $+1$ if the O lies in this upper right quadrant and the X does not, and it contributes -1 if the X lies in this upper right quadrant and the O does not, and it contributes 0 otherwise; i.e.

$$\#(p_+ \cap \mathcal{D}) = \mathcal{I}(p, \mathbb{O} - \mathbb{X}).$$

Similarly, the intersection number of the ray p_- from p to $(-\infty, y)$ with $\mathcal{D}$ is

$$\#(p_- \cap \mathcal{D}) = \mathcal{I}(\mathbb{O} - \mathbb{X}, p).$$

Clearly, $w_{\mathcal{D}}(p) = \#(p_+ \cap \mathcal{D}) = \#(p_- \cap \mathcal{D})$. Average the above two equations to get Equation (4.24). □

Fix a planar realization of a toroidal grid diagram, and consider the function A' on the grid state $\mathbf{x} \in \mathbf{S}(\mathbb{G})$ defined by

$$A'(\mathbf{x}) = -\sum_{x \in \mathbf{x}} w_{\mathcal{D}}(x). \tag{4.25}$$

As we shall see shortly, A and A' differ by a constant (independent of the grid state). We express this constant in terms of quantities which we have met already in Section 3.3. To this end, recall that each of the $2n$ squares marked with an X or O has 4 corners, giving us a total of $8n$ lattice points on the grid (possibly counted with multiplicity, when the marked squares share a corner), which we denote $p_1, \ldots, p_{8n}$. The sum of the winding numbers at these points, divided by 8, was denoted by $a(\mathbb{G})$ in Section 3.3. The precise relationship between A and A' can now be stated as follows:

PROPOSITION 4.7.2. *Choose a planar realization of a toroidal grid diagram $\mathbb{G}$ representing a knot K. Let $\mathcal{D}$ be the corresponding diagram of K. The Alexander function A can be expressed in terms of the winding numbers $w_{\mathcal{D}}$ by the following formula:*

$$A(\mathbf{x}) = -\sum_{x \in \mathbf{x}} w_{\mathcal{D}}(x) + \frac{1}{8}\sum_{j=1}^{8n} w_{\mathcal{D}}(p_j) - \left(\frac{n-1}{2}\right) = A'(\mathbf{x}) + a(\mathbb{G}) - \frac{n-1}{2}. \tag{4.26}$$

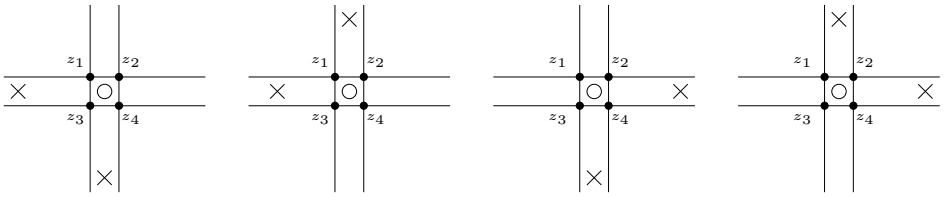

FIGURE 4.7. **Verification of Equation** (4.28)**.** Here are the four cases where the distinguished square z is marked with an O. To verify the equation, find the pairs contributing to $\mathcal{J}(z_1 + \cdots + z_4, X)$, where X is in the same row or column as z, and to $\mathcal{J}(z_1 + \cdots + z_4, O)$, where the O-marking is at z.

Proof. Summing Equation (4.24) over all the components $x \in \mathbf{x}$, gives $A'(\mathbf{x}) = -\mathcal{J}(\mathbf{x}, \mathbb{O} - \mathbb{X})$; so

$$\begin{aligned} A(\mathbf{x}) &= \frac{1}{2}(M_{\mathbb{O}}(\mathbf{x}) - M_{\mathbb{X}}(\mathbf{x})) - \left(\frac{n-1}{2}\right) \\ &= -\mathcal{J}(\mathbf{x}, \mathbb{O} - \mathbb{X}) + \frac{1}{2}(\mathcal{J}(\mathbb{O}, \mathbb{O}) - \mathcal{J}(\mathbb{X}, \mathbb{X})) - \left(\frac{n-1}{2}\right) \\ &= A'(\mathbf{x}) + \frac{1}{2}\mathcal{J}(\mathbb{O} + \mathbb{X}, \mathbb{O} - \mathbb{X}) - \left(\frac{n-1}{2}\right). \end{aligned}$$

Thus, Equation (4.26) now follows once we show that

$$\frac{1}{2}\mathcal{J}(\mathbb{O} + \mathbb{X}, \mathbb{O} - \mathbb{X}) = \frac{1}{8}\sum_{i=1}^{8n} w_{\mathcal{D}}(p_i). \tag{4.27}$$

To check Equation (4.27), we first verify the following: given any small square (in a planar grid) whose center z is marked with an O or an X, if $z_1, \ldots, z_4$ denote its four corner points in the plane, then

(4.28)

$$\mathcal{J}(z, \mathbb{O} - \mathbb{X}) = \frac{1}{4}\mathcal{J}(z_1 + z_2 + z_3 + z_4, \mathbb{O} - \mathbb{X}) + \begin{cases} -\frac{1}{4} & \text{if } z \text{ is marked with an } O \\ \\ \frac{1}{4} & \text{if } z \text{ is marked with an } X. \end{cases}$$

Suppose for definiteness that z is marked with an O. Then, for any marking $O' \in \mathbb{O}$ with $O \neq O'$,

$$\mathcal{J}(z, O') = \frac{1}{4}\mathcal{J}(z_1 + z_2 + z_3 + z_4, O').$$

Also, for any X-marking not in the same row or column as z,

$$\mathcal{J}(z, X) = \frac{1}{4}\mathcal{J}(z_1 + z_2 + z_3 + z_4, X).$$

The correction of $-\frac{1}{4}$ comes from the pairing of the X-markings in the same row and column as z with the formal sum $z_1 + \cdots + z_4$, combined with the pairing of the O-marking on z with $z_1 + \cdots + z_4$; see Figure 4.7. A similar reasoning gives Equation (4.28) when z is marked with an X.

Equation (4.27) follows from summing up Equation (4.28) over all O- and X-marked squares, and using Lemma 4.7.1. □

LEMMA 4.7.3. *The sign of the permutation that connects* $\mathbf{x}$ *with* $\mathbf{x}^{NWO}$ *is* $(-1)^{M(\mathbf{x})}$.

Proof. This is an immediate consequence of Proposition 4.3.1, combined with the mod 2 reductions of Equations (4.1) and (4.2). □

DEFINITION 4.7.4. Let $X = \bigoplus_{d,s} X_{d,s}$ be a bigraded vector space. Define the ***graded Euler characteristic of*** X to be the Laurent polynomial in t given by

$$\chi(X) = \sum_{d,s} (-1)^d \dim X_{d,s} \cdot t^s.$$

The Euler characteristic of grid homology is related to the Alexander polynomial, according to the following:

PROPOSITION 4.7.5. *Let* $\mathbb{G}$ *be a grid diagram for a knot* K *with grid number* n. *The graded Euler characteristic of the bigraded vector space* $\widetilde{GH}(\mathbb{G})$ *is given by*

$$\chi(\widetilde{GH}(\mathbb{G})) = (1-t^{-1})^{n-1} \cdot \Delta_K(t), \tag{4.29}$$

where $\Delta_K(t)$ *is the symmetrized Alexander polynomial of Equation* (2.3).

Proof. It is a standard fact that the Euler characteristic of a chain complex agrees with that of its homology (and this fact remains true in the bigraded case). Thus,

$$\chi(\widetilde{GH}(\mathbb{G})) = \chi(\widetilde{GC}(\mathbb{G})) = \sum_{\mathbf{x} \in \mathbf{S}(\mathbb{G})} (-1)^{M(\mathbf{x})} t^{A(\mathbf{x})}.$$

By Proposition 4.7.2 (for the t-power) and Lemma 4.7.3 together with Proposition 4.3.7 (for the sign), it follows that this graded Euler characteristic agrees with

$$\sum_{\mathbf{x}} (-1)^{M(\mathbf{x})} t^{A(\mathbf{x})} = (-1)^{n-1} \epsilon(\mathbb{G}) \cdot \det(\mathbf{M}(\mathbb{G})) \cdot t^{a(\mathbb{G})} \cdot t^{\frac{1-n}{2}}.$$

The result now follows from Theorem 3.3.6. □

Proposition 4.7.5 relates the Euler characteristic of $\widetilde{GH}(\mathbb{G})$ and the Alexander polynomial of the underlying knot. This leads quickly to the following relationship between the Alexander polynomial and the graded Euler characteristic of $\widehat{GH}$

$$\chi(\widehat{GH}(K)) = \sum_{d,s} (-1)^d \dim\ \widehat{GH}_d(K,s) \cdot t^s \in \mathbb{Z}[t,t^{-1}]. \tag{4.30}$$

THEOREM 4.7.6 ([**172, 191**]). *The graded Euler characteristic of the simply blocked grid homology is equal to the (symmetrized) Alexander polynomial* $\Delta_K(t)$*:*

$$\chi(\widehat{GH}(K)) = \Delta_K(t).$$

Proof. The graded Euler characteristic of the bigraded vector space W from Lemma 4.6.15 is $\chi(W) = 1 - t^{-1}$, so the identity follows immediately from Propositions 4.7.5 and 4.6.15. □

4.8. Computations

Assuming Theorem 4.6.19, we can directly compute some of the homology groups defined earlier in this chapter. See also Chapter 10 for more computations.

PROPOSITION 4.8.1. *For the unknot $\mathcal{O}$, $\widehat{GH}(\mathcal{O}) \cong \mathbb{F}$ is supported in bigrading $(0,0)$; and $GH^-(\mathcal{O}) \cong \mathbb{F}[U]$, and its generator has bigrading $(0,0)$.*

Proof. In the 2×2 grid diagram $\mathbb{G}$ representing the unknot, there are exactly two generators; call them $\mathbf{p}$ and $\mathbf{q}$, with $A(\mathbf{p}) = 0$, $M(\mathbf{p}) = 0$, $A(\mathbf{q}) = -1$, $M(\mathbf{q}) = -1$. The complex $GC^-(\mathbb{G})$ is generated over $\mathbb{F}[V_1, V_2]$ by these two generators, and its boundary map is specified by

$$\partial^-_{\mathbb{X}}(\mathbf{p}) = 0, \qquad \partial^-_{\mathbb{X}}(\mathbf{q}) = (V_1 + V_2) \cdot \mathbf{p}.$$

The homology of this complex is clearly isomorphic to $\mathbb{F}[U]$, generated by the cycle $\mathbf{p}$; this completes the computation of $GH^-(\mathcal{O})$.

For $\widehat{GH}(\mathcal{O})$, we can set $V_2 = 0$, to obtain the complex over $\mathbb{F}[V_1]$ with generators $\mathbf{p}$ and $\mathbf{q}$, and boundary specified by

$$\partial^-_{\mathbb{X}}(\mathbf{p}) = 0, \qquad \partial^-_{\mathbb{X}}(\mathbf{q}) = V_1 \cdot \mathbf{p},$$

whose homology is $\mathbb{F}$, generated by the cycle $\mathbf{p}$. □

With more work, one can show that the grid homology groups of the right-handed trefoil knot $K = T_{2,3}$ are given by:

$$\widehat{GH}_d(K,s) = \begin{cases} \mathbb{F} & \text{if } (d,s) \in \{(0,1),(-1,0),(-2,-1)\} \\ 0 & \text{otherwise.} \end{cases} \tag{4.31}$$

$$GH^-_d(K,s) = \begin{cases} \mathbb{F} & \text{if } (d,s) = (0,1) \text{ or } (d,s) = (-2k,-k) \text{ for } k \geq 1 \\ 0 & \text{otherwise.} \end{cases} \tag{4.32}$$

In the second case, the $\mathbb{F}[U]$-module structure is determined by the property that $U\colon GH^-_{-2k}(K,-k) \to GH^-_{-2k-2}(K,-k-1)$ is an isomorphism for all $k \geq 1$. More succinctly, we write

$$GH^-(K) \cong (\mathbb{F}[U]/U)_{(0,1)} \oplus (\mathbb{F}[U])_{(-2,-1)},$$

where the subscripts on the cyclic $\mathbb{F}[U]$-modules denote the bigradings of their generators.

EXERCISE 4.8.2. Let K denote the right-handed trefoil knot.
(a) Use Figure 3.3 to verify Equation (4.31). (*Hint:* Show first that there are no generators for $\widehat{GC}(\mathbb{G})$ in Alexander grading greater than 1. Next, find generators of $\widehat{GC}(\mathbb{G})$ in Alexander gradings 0, 1, and -5, and apply Proposition 4.6.15.)
(b) Verify Equation (4.32). (*Hint:* Proposition 4.6.18 might be helpful.)
(c) Let K denote the left-handed trefoil knot. Compute $\widehat{GH}(K)$ and $GH^-(K)$.

REMARK 4.8.3. The result of Exercise 4.8.2 shows that grid homology distinguishes the right-handed trefoil $T_{2,3}$ from its mirror $T_{-2,3}$. See Proposition 7.1.2 for a general description of how homology behaves under reflection.

Restricting attention to a carefully chosen Alexander grading, we can give a more general computation valid for all torus knots.

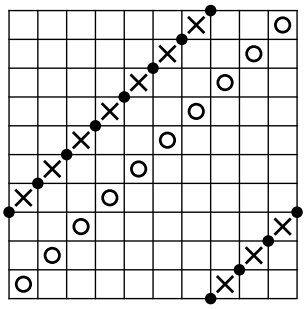

FIGURE 4.8. **Grid diagram for $T_{-3,7}$.** This is the diagram for $T_{-p,q}$ from Exercise 3.1.5(c), when $p = 3$ and $q = 7$. The grid state $\mathbf{x}^+$ is indicated by the heavy dots in the grid.

LEMMA 4.8.4. *Let $p, q > 1$ be relatively prime integers. There is a grid diagram $\mathbb{G}$ for $T_{-p,q}$ with the following property. If $\mathbf{x}^+ = \mathbf{x}^{NEX}$ is the grid state which occupies the upper right corner of each square marked with X, then this grid state is the unique generator with maximal Alexander grading among all generators, and*

$$A(\mathbf{x}^+) = \frac{(p-1)(q-1)}{2}.$$

Proof. Let $\mathbb{G}$ be the $(p+q) \times (p+q)$ grid diagram with $\sigma_{\mathbb{O}} = (1, \ldots, p+q)$ and $\sigma_{\mathbb{X}} = (p+1, p+2, \ldots, p)$; see Figure 4.8. (Compare also Exercise 3.1.5(c)).

Consider the associated winding matrix $M_{p,q} = \mathbf{W}(\mathbb{G})$. In the j^{th} row, the winding numbers start out zero for a while, they increase by 1's until they reach their maximum, then they stay constant, and then eventually they drop by 1's. More precisely: the left column and bottom row vanish; for $j = 1, \ldots, q$, in the j^{th} row (from the top), the first $q - j + 1$ entries are 0 and all others are positive; while for $j = q+1, \ldots, p+q-1$, the last $j - q$ entries and the first entry are 0 and all others are positive.

For example, for the torus knot $T_{-3,7}$ from Figure 4.8, this matrix is

$$M_{3,7} = \begin{pmatrix} 0 & 0 & 0 & 0 & 0 & 0 & 0 & 1 & 1 & 1 \\ 0 & 0 & 0 & 0 & 0 & 0 & 1 & 2 & 2 & 1 \\ 0 & 0 & 0 & 0 & 0 & 1 & 2 & 3 & 2 & 1 \\ 0 & 0 & 0 & 0 & 1 & 2 & 3 & 3 & 2 & 1 \\ 0 & 0 & 0 & 1 & 2 & 3 & 3 & 3 & 2 & 1 \\ 0 & 0 & 1 & 2 & 3 & 3 & 3 & 3 & 2 & 1 \\ 0 & 1 & 2 & 3 & 3 & 3 & 3 & 3 & 2 & 1 \\ 0 & 1 & 2 & 2 & 2 & 2 & 2 & 2 & 1 & 0 \\ 0 & 1 & 1 & 1 & 1 & 1 & 1 & 1 & 0 & 0 \\ 0 & 0 & 0 & 0 & 0 & 0 & 0 & 0 & 0 & 0 \end{pmatrix}.$$

It follows at once that for $\mathbf{x}^+$ all the winding numbers are zero, and for all other grid states $\mathbf{x}$, the sum of the winding numbers $-A'(\mathbf{x})$ is positive; so by Proposition 4.7.2, $\mathbf{x}^+$ is the unique grid state with maximal Alexander grading.

Elementary computation shows that

$$\mathcal{J}(\mathbf{x}^+,\mathbf{x}^+)=\frac{p(p-1)+q(q-1)}{2} \qquad \mathcal{J}(\mathbb{O},\mathbb{O})=\frac{(p+q)(p+q-1)}{2}$$
$$\mathcal{J}(\mathbf{x}^+,\mathbb{O})=\frac{p^2+q^2}{2} \qquad M_{\mathbb{X}}(\mathbf{x}^+)=1-p-q;$$

so using Definition 4.3.2 we find that

$$A(\mathbf{x}^+)=\frac{1}{2}(M_{\mathbb{O}}(\mathbf{x}^+)-M_{\mathbb{X}}(\mathbf{x}^+))-\frac{p+q-1}{2}=\frac{(p-1)(q-1)}{2}.$$

□

PROPOSITION 4.8.5. *Fix relatively prime, positive integers p and q with $p,q>1$. Some of the grid homology groups $\widehat{GH}(T_{-p,q})$ are given by the following:*

$$\widehat{GH}_d(T_{-p,q},s)=\begin{cases}\mathbb{F} & \text{if } s=\frac{(p-1)(q-1)}{2} \text{ and } d=(p-1)(q-1)\\ 0 & \text{if } s=\frac{(p-1)(q-1)}{2} \text{ and } d\neq(p-1)(q-1)\\ 0 & \text{if } s>\frac{(p-1)(q-1)}{2}.\end{cases}$$

Proof. According to Lemma 4.8.4, $\widehat{GC}(T_{-p,q})$ has no generators with Alexander grading greater than $\frac{(p-1)(q-1)}{2}$; and it has a single one with Alexander grading equal to $\frac{(p-1)(q-1)}{2}$. The formulas in the proof of Lemma 4.8.4 also show that $M(\mathbf{x}^+)=(p-1)(q-1)$. □

To give further examples, we find it convenient to encode the grid homology by its Poincaré polynomial $P_K(q,t)=\sum_{d,s}\dim\ \widehat{GH}_d(K,s)t^sq^d$ (introduced in Equation (1.2)). Using a direct computer computation, Baldwin and Gillam [**5**] computed the grid homology of all knots with at most twelve crossings. In particular, for the eleven crossing Kinoshita-Terasaka knot KT and for its Conway mutant C of Figure 2.7 (compare also [**182**, Section 5.4] and [**179**, Section 3]) they found that:

$$P_{KT}(q,t)=(q^{-3}+q^{-2})t^{-2}+4(q^{-2}+q^{-1})t^{-1}+6q^{-1}+7+4(1+q)t+(q+q^2)t^2, \tag{4.33}$$

$$P_C(q,t)=(q^{-4}+q^{-3})t^{-3}+3(q^{-3}+q^{-2})t^{-2}+3(q^{-2}+q^{-1})t^{-1}+2q^{-1}$$
$$+3+3(1+q)t+3(q+q^2)t^2+(q^2+q^3)t^3. \tag{4.34}$$

(Among non-trivial knots with at most eleven crossings, these are the two knots with Alexander polynomial equal to 1.)

Although these are not computations one would wish to perform by hand, there are pieces which can be verified directly. For example:

EXERCISE 4.8.6. Consider Figure 4.9, a grid diagram for the Conway knot.
(a) Show that the grid states pictured on the figure are the only two grid states in Alexander grading 3, and that there are no grid states in greater Alexander grading.
(b) Show that there are no empty rectangles connecting the two grid states. Use this to verify that the coefficient in front of the t^3 term in the Poincaré polynomial $P_C(q,t)$ of the Conway knot is, indeed, (q^2+q^3), as stated in Equation (4.34), and that all higher t-powers have vanishing coefficients.

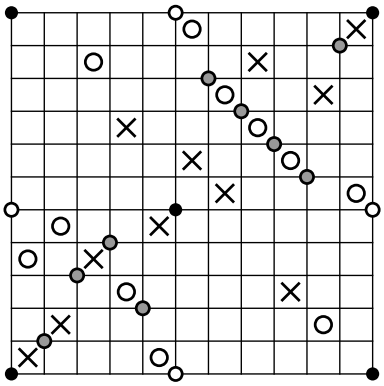

FIGURE 4.9. **Two grid states for the Conway knot.** The white ones appear only in one of the grid states, the black ones appear only in the other, and the gray dots appear in both.

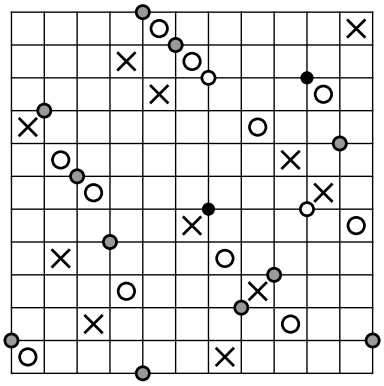

FIGURE 4.10. **Two grid states for the Kinoshita-Terasaka knot.** We have exhibited here two grid states on the same grid, with the same conventions as in Figure 4.9.

EXERCISE 4.8.7. Consider the grid diagram of the Kinoshita-Terasaka knot KT from Figure 4.10. (Notice that the diagram for the Kinoshita-Terasaka knot we gave in Figure 3.4 differs from this diagram by a single commutation.)
(a) Show that there are exactly four grid states in Alexander grading 2, and none with Alexander grading greater than 2. (*Hint:* Two of the grid states in Alexander grading 2 are pictured in Figure 4.10. Find the other two.)
(b) Show that the homology of the resulting chain complex in Alexander grading 2 has dimension 2. Use this to verify that the coefficient in front of t^2 in $P_{KT}(q,t)$ is (q^2+q^1), and all coefficients with higher t-powers vanish, as stated in Equation (4.33).

REMARK 4.8.8. For a typical grid diagram of the Kinoshita-Terasaka knot with grid number 11, the number of generators in Alexander grading 2 is rather large. For

the choice we gave here, there are four generators, and this makes the computation of the grid homology in this Alexander grading easy.

4.9. Further remarks

The argument from Lemma 4.6.7 is a combinatorial analogue of the proof, in Lagrangian Floer homology, that the Lagrangian Floer complex is, in fact, a chain complex. The proof in that case hinges on Gromov's compactness theorem, together with gluing results for solutions of the relevant non-linear Cauchy-Riemann operator. These results are key ingredients in the development of Lagrangian Floer homology. Likewise, the combinatorial arguments from Lemma 4.6.7, although they are much simpler, also lie at the core of grid homology. Arguments of this type will appear throughout the text. (See for example Lemma 4.6.9 and Lemma 5.1.4.)